Endothelialisation of Polyvinyl Alcohol Small Diameter Vascular Graft

by

Grace Pohan

A thesis
presented to the University of Waterloo
in the fulfillment of the
thesis requirements for the degree of
Master of Applied Science
in
Chemical Engineering

Waterloo, Ontario, Canada, 2018
© Grace Pohan 2018

AUTHOR'S DECLARATION

This thesis consists of material all of which I authored or co-authored: see Statement of Contributions included in the thesis. This is a true copy of the thesis, including any required final revisions, as accepted by the examiners.

I understand that my thesis may be made electronically available to the public.

STATEMENT OF CONTRIBUTIONS

Chapter 3 in this thesis is co-authored with Ms. Sabrina Mattiassi from Chemical Engineering department, University of Waterloo whom I mentored during her co-op term in Yim lab. The data presented in Chapter 3 for uniaxial tensile test, burst pressure test, and suture retention test were done together with Ms. Mattiassi. Compliance test, bend radius and contact angle test were performed solely by Ms. Mattiassi. Data analysis of the above tests was done by Ms. Mattiasi.

ABSTRACT

As one of the possible treatments for cardiovascular disease (CVD), bypass grafting in small diameter vessel (≤ 6 mm diameter) is often employed. However, maintaining the patency of this small diameter graft remains a challenge despite 50 years of research in this area. While ePTFE graft performance as a large diameter vascular graft is commendable and has been widely used in patients, the performance of ePTFE small diameter vascular graft is disappointing with 65% graft patency rate at 1 year.[1] It was observed that graft occlusion is caused mainly by thrombus or intima hyperplasia (IH) formation. This study proposes the use of sodium trimetaphosphate (STMP) crosslinked polyvinyl alcohol (PVA) as small diameter vascular graft due to its low thrombogenicity and excellent mechanical property. However, PVA hydrophilicity is known to hinder any extracellular matrix (ECM) protein or cell attachment on its surface, while surface endothelialisation is believed to prevent thrombus and IH formation. We hypothesize that NH_3 plasma luminal modification on the luminal surface of PVA along with hydrogel patterning with microtopography can improve surface interaction with endothelial cells. Additionally, we speculate the effect of terminal sterilization step on PVA grafts is minimum and the grafts can maintain its patency at 28 to 30-day timepoint.

Endothelial cell attachment on PVA surface was found to improve on plasma treated luminal surface with 2 μm gratings topography. Endothelial gene expressions (PECAM1 and NOS3) were, however, found to be downregulated on plasma treated substrates. However, platelet and fibrin activation of the microgratings topography done with baboon ex vivo shunt model was comparable or lower than ePTFE graft control and collagen coated glass conduit. Furthermore,

sterilization of PVA graft with γ-radiation was not found to have any toxic effect on cells and interestingly improve endothelialisation. While EtO sterilization was shown to alter PVA mechanical and material properties, γ-radiation only affected PVA graft mechanical compliance. Gamma irradiated small diameter PVA graft (2 mm ID) without any surface topography was implanted with end-to-side anastomoses at the right common carotid artery to assess PVA performance over 28-30 days in rabbit models. Five out of 7 PVA grafts were found patent after 28-30 days of implantation, while only 1 out of 2 ePTFE grafts were patent after 28-30 days. Endothelialisation of PVA graft in vivo was, however, not yet observed which compels the importance of plasma treatment and topography incorporation in the future work.

ACKNOWLEDGEMENTS

I would like to express my sincerest gratitude to my supervisor, Associate Professor Evelyn Yim, for her enormous support and advice throughout this Master's program. Her patience and trust are what keeping me motivated to obtain the best possible outcome in my research.

I would like to also thank the thesis committee members, Professor Ting Tsui and Associate Professor Boxin Zhao for the constructive criticism and suggestions which help to improve the content of this thesis.

I would like to extend my appreciation to Dr. Monica Hinds and Dr. Deirdre Anderson (Oregon Health and Science University, Portland) for running ex vivo shunt study to check the platelet and fibrin activation on PVA surfaces, to Dr. Diego Mantovani and Dr. Pascale Chevalier (Laboratory for Biomaterials and Bioengineering, CRC-I, CHU de Québec Research Center, Laval University, and CHU Research Center of Quebec) for plasma treating PVA grafts and running XPS, to Mr. John Tse for taking IF images for the cell adhesion study, to Associate Professor Boxin Zhao for giving permission to use the tribometer and water contact angle instrument, to Associate Professor Alfred Yu, Dr. Adrian Chee, and Mr. Billy Yat Shun Yiu for taking the ultrasound measurements in the in vivo work of this study, and to Dr. Filip Konecny and all CAF AHT who have been involved in the surgery and who have been great teachers in caring and handling of the animals. I would also like to thank all members of Yim lab who have been helping in the in vivo work, be it sample collection, surgery minutes taking, instruments cleaning, and post-op care; I treasure the friendship we had during my time in the laboratory.

Last but not least, I would like to thank God, my parents, my brother, my fiancé, my sister-in-law, and my friends whose love has been a source of great encouragement and who are always there in all the ups and downs of life.

TABLE OF CONTENTS

LIST OF FIGURES

LIST OF TABLES

LIST OF ABBREVIATIONS

CAM : Cell Adhesion Molecule

CVD : Cardiovascular Diseases

EtO : Ethylene Oxide

ID : Internal Diameter

IH : Intimal Hyperplasia

NaOH : Sodium Hydroxide

ePTFE : Expanded Polytetrafluoroethylene

PDMS : Polydimethylsiloxane

PHZ : Para anastomotic Hypercompliant Zone

PTFE : Polytetrafluoroethylene

PVA : Polyvinyl Alcohol

STMP : Sodium Trimetaphosphate

CHAPTER 1

Introduction and Literature Review

1.1 Cardiovascular disease (CVD) and disease treatment

Cardiovascular diseases (CVD) are the number one cause of death globally.[2] Two leading types of CVD, ischaemic heart disease and stroke have affected more than 8 million people in 2015. The early pathology of ischaemic heart disease and stroke begins with a condition called atherosclerosis where lipid, cholesterol, and other substances in the blood circulation accumulate and form a plaque which eventually causes obstruction to the blood flow. Surrounding tissues that do not receive enough oxygen and will eventually die (ischemia) and depending on what type of tissues is affected, it can lead to other cardiovascular diseases. In the case of ischaemic heart disease and stroke, the tissues experiencing ischemia are heart and brain tissues respectively.

There are 2 treatments that are commonly performed to reduce vessel stenosis and to increase blood flow. The first treatment called angioplasty and stenting is a way to push the plaque onto the vessel wall by using an inflated balloon and a vascular stent which are inserted through a catheter. The treatment is slightly invasive and is preferred at mild CVD stage. It is noted, however, that due to various factors including lifestyle and genetics, the restenosis of the vessel lumen can happen. The restenosis can be caused by new plaque build up or neointima formation due to scar at the internal vessel wall created by the assembled stent. In a more severe case (multiple vascular occlusions along the vessel), however, angioplasty and stenting are not feasible to be done. The second treatment option to tackle the vessel obstruction is through implantation of vascular graft that bypass the blocked area in the vessel.

The gold standard of vascular graft remains the autologous graft which possesses matching physiological properties with the surrounding native vessels. However, autologous graft is limited in availability and the use of this graft type creates relatively milder injury at the donor site. With this consideration, cryopreserved homograft from cadaver became an alternative option

to autologous graft. As in any other biological vascular grafts outside autologous graft, homograft imposes immunogenic concern which requires patients to take a continuous dose of immunosuppressant. More importantly, a study shows that the Young's modulus of homograft is altered due to cryopreservation of the blood vessel[3]. Due to the complexity in the homograft cryopreservation, this option was abandoned by many in 1960s. Meanwhile, allograft (same source species) and xenograft (different source species) have similar concern pertaining to immunogenic reaction and disruption of vascular intima fiber upon decellularization[4]. Also, without re-endothelialisation of the decellularized graft, the extra-cellular matrix left behind is likely to be platelet-activating. Due to these limitations, the development of synthetic vascular graft has, therefore, attracted clinicians' attention. The preparation of synthetic vascular graft is in general faster (eliminating the need of donor) and less costly, especially in a large-scale fabrication, providing an off the shelf option for a vascular graft.

1.2 Factors influencing the development of thrombus and intimal hyperplasia in vivo

As any other bypass graft implants, synthetic vascular grafts also face pathological issue called intimal hyperplasia (IH) where smooth muscle cells proliferate and create layers of intima tissue which lead to stenosis of graft starting from the anastomosis region. IH is believed to be caused by shear stresses against the vessel wall (oscillatory shear stress, shear stress gradient, turbulence) and vessel wall injury that gives signal to the endothelial cells to trigger the migration and proliferation of smooth muscle cells into the lumen.[5] In bypass vascular graft application, IH is usually formed at the anastomosis between graft and vessel. Not only does the bypass graft configuration create a flow bifurcation and hence an increase in wall shear stress on the internal side of the bifurcation, but also this configuration magnifies the mechanical compliance/ distensibility mismatch between native vessel and graft materials, creating concentrated stress

along the suture line at the graft anastomoses and vascular injury.[6] The first cause of IH is, however, unavoidable because it is technically simpler to implant graft with an end-to-side anastomosis configuration rather than with an end-to-end anastomosis configuration and disturb the native vessel pre-tension too much, especially in a multiple artherosclerosis case along the vessel. The second IH cause (mechanical compliance mismatch) is what most vascular graft researchers are studying and trying to achieve. In fact, ePTFE small diameter graft failure is believed to be mainly caused by its high stiffness.[7]

In addition to IH, synthetic vascular grafts can also be clogged by thrombus when implanted. According to Rudolf Virchow's triad, there are three factors that affect thrombogenesis; these include circulatory stasis, vascular wall injury, and hypercoagulable state.[8] The first factor, circulatory stasis, refers to the hemodynamic in blood vessels whereby irregularity in blood flow (oscillatory flow) can cause the deposition of plaque at the vessel wall and the subsequent plaque rupture which causes thrombus formation. One example of this would be plaque deposition at carotid sinus near the bifurcation. The increase in vessel volume at the sinus causes a sudden pressure-drop and creates an oscillatory flow region. Moreover, arrhythmia patients are known to have higher chance of forming thrombus in their vessel. The second factor, vascular wall injury, refers to the injury mainly caused by surgical intervention, for example, bleeding after the anastomosing of a vascular graft to the native vessel, or after having hemodialysis puncture. The last factor, hypercoagulable state, refers to abnormal state of the blood coagulation cascade caused by anomaly of blood platelet or of fibrinolysis process.[9] This state can also be caused by an increased level of estrogen in blood or by inflammation in some body parts. From the three Virchow's triad factors, the first two factors are the more common factors in promoting thrombogenesis.

Both IH and thrombus problems are more critical in small diameter vascular graft bypass where a small degree of stenosis can cause a complete lumen obstruction and a graft failure.

1.3 Endothelial cell functions and importance in vascular graft application

In blood vessels, endothelial cells lining functions as a barrier between blood and the outside environment, and depending on where the vessel is located, these cells may be surrounded by layers of elastic tissue, smooth muscle cells, and fibrous tissue. As a barrier, endothelial cells regulate hemostasis which means maintaining the stability of blood circulation through activating coagulation process in case of injury.[10] These cells are responsible to send signal to platelet to form an initial platelet plug at the injured area and to coagulation factors which activate fibrinogen to become fibrin and strengthen the plug forming a clot tissue. In a normal condition, through sensing the increase in wall shear stress, endothelial cell secretes nitric oxide (NO) to cause smooth muscle cells underlying them to relax and subsequently dilate vessel diameter.[11] Moreover, endothelial cells control the proliferation and migration of the smooth muscle cells by secreting enzyme and inhibitors to the enzyme.[12] The presence of endothelial cells lining also prevents the activation of platelet and subsequent thrombogenesis.

Promoting endothelialisation on the vascular graft lumen, therefore, becomes one of the main focus in vascular engineering research and goes hand-in-hand with the improvement of graft mechanical compliance to match native vessel compliance.

1.4 Small diameter expanded polytetrafluoroethylene (ePTFE) vascular graft

ePTFE was discovered in 1969 and has a better tensile strength compared to the high-density PTFE. Due to its high porosity, the production of ePTFE is less costly. ePTFE can be manufactured through polymerization of C_2F_4 monomer with the addition of peroxide. Because it

is biologically inert, biocompatible, and it can be made into tubular shape, ePTFE is used to fabricate vascular grafts for over 30 years. The use of ePTFE as vascular graft is notably decent in patency for large diameter vascular graft (graft inner diameter > 6 mm); however, the patency of small diameter ePTFE vascular graft still requires improvement.

Due to the rigidity of ePTFE material, kinking is a problem for this graft in the early days. Kinking at the graft will cause flow disturbance and lead to thrombus formation and subsequent graft failure. Gore-Tex came up with stretch ePTFE grafts with higher degree of conformability and resistance to kinking and a study was conducted in 1992 to test the patency of stretch ePTFE grafts. Thirty-seven patients were involved in the study where 17 patients received standard small diameter ePTFE grafts and the remaining 20 received stretch ePTFE grafts. Two of the standard ePTFE grafts were occluded within 24 h of operation and two stretch ePTFE grafts were occluded after 2 and 5 months. Although stretch ePTFE grafts have higher patency than standard ePTFE grafts, the primary patency of both types after 1 year of implantation are low (59% for stretch ePTFE graft and 29% for standard ePTFE graft).[13]

Another commonly seen problem in an ePTFE graft is stenosis of the graft lumen at the sutured area due to neointima formation which leads to intimal hyperplasia. Neointima is believed to be caused by smooth muscle cell proliferation in response to an increase in wall stresses at the suture line; the cell proliferation is then followed by angiogenesis into the mass. When the stenosis is reaching about 50% of the lumen, an endovascular intervention with angioplasty is usually performed to reopen the lumen wider. However, study has documented the recurrence of stenosis 5 months after the treatment.[14]

1.5 Other synthetic materials for making small diameter vascular grafts

With the current limitation of small diameter ePTFE vascular grafts, other polymers and composite materials were explored including poly(ε-caprolactone) (PCL),[4, 15-16] polyurethane (PU),[17-19] poly(vinyl) alcohol (PVA),[20-23] silk fibroin,[24-27] poly(L-lactic acid) (PLA).[28-33] Moreover, existing ePTFE graft was also modified with extracellular matrix protein such as heparin to improve its patency rate.[34-36] The properties of the vascular graft materials based on the cited papers above are summarized in the following table and is compared to the golden standard (femoral artery):

Table 1. Vascular graft material properties for making small diameter graft

Material	Biocompatibility	Compliance compatibility	Cell infiltration/ migration	Cost-effectiveness	Biodegradability
Hep- ePTFE	√	-	√	-	-
PCL	√	-	√	√	√
PU	√	√	-	√	-
PVA	√	√	-	√	-
Silk fibroin	√ (potential allergen)	-	√	√	√
PLA	√	-	-	√	√
Femoral artery	√	√	√	NA	-

Additionally, Thomas et al.[37] summarized the ideal vascular graft criteria as follows:

- Infection-resistant
- Biocompatible (noninflamatory, nontoxic, noncarcinogenic, nonimmunogenic).

- Nonthrombogenic and acquire certain level of porosity to prevent leakage but can serve as selective permeable diffusion barrier
- Capable to match blood vessel mechanical properties (strength, compliance, suture retention, burst pressure, kink resistant)
- Acquire vasoactive physiological properties to allow constriction and relaxation of graft in the presence of neural or chemical stimuli
- Practical in fabrication technique and cost-effective to allow for large scale fabrication in order to meet the demand.

At the current state, none of the vascular graft materials can fully meet all the mentioned criteria. However, it is important to note that what considers a critical property in one graft material may not be required in other small diameter vascular graft applications as different implantation site of the small diameter vascular graft may have different requirement, e.g. graft length and mechanical property. Our group is particularly interested in utilizing PVA hydrogel as small diameter graft material due to its excellent mechanical property tunability and the ease of its fabrication over PU.

1.6 Polyvinyl alcohol hydrogel properties

Polyvinyl alcohol (PVA) is a hydrogel material, rich in –OH function group and can be produced from base hydrolization of polyvinyl acetate ester function group. The hydrolization percentage of PVA determines the polymer chain conformation in solvent such as water because –OH function group is hydrophilic while $–OCOCH_3$ function group is hydrophobic. In a fully hydrolized PVA where there is no presence of $–OCOCH_3$ function group, the polymer is highly soluble in water and has a high packing density.

To use PVA for medical application, the polymer has to be first crosslinked in order to obtain the desirable mechanical integrity. PVA can be physically crosslinked with freeze-thaw method or photo-crosslinking method with UV-radiation in the presence of sensitizer, or chemically crosslinked through reaction with its –OH function group with the addition of toxic chemical such as glutaraldehyde. Lately, a study has also shown the use of safe food grade crosslinker such as sodium trimetaphosphate (STMP) to make crosslinked PVA polymer with good mechanical property.[20] All of the crosslinked PVA is water-insoluble.

In freeze-thaw method, PVA solution is cooled to -20^{o}C and thawed back to room temperature for a few times. The physical crosslinking of PVA can happen due to the formation of crystalline regions during this process. Crosslinked PVA with freeze-thawed method exhibits a higher degree of swelling in water.[38] However, one disadvantage of crosslinking PVA with freeze-thaw method is the dissolution of some of the uncrosslinked or weakly crosslinked polymer chain into the solvent during swelling.[39] Its Young's modulus is also generally lower than the chemically crosslinked PVA.[40]

In photo-crosslinking method, the crosslinking of PVA is done with UV-radiation which requires the presence of sensitizer such as sodium benzoate. Photolysis of sensitizer provides a radical that abstract a tertiary hydrogen atom from the polymer chain, yielding to a polymeric radical. This polymeric radical will then react with the –OH groups and form ether bonds between the polymer chains.[41]

Furthermore, in chemical crosslinking method, glutaraldehyde in alcoholic solution can be used to chemically crosslink PVA; generally, in the presence of acid such as HCl or H_2SO_4. The swelling of PVA by the alcoholic solvent promotes the diffusion of glutaraldehyde and protonic

ions; the latter catalyzes the crosslinking reaction.[42-43] Subsequently, a study in 2008 has shown the possibility of creating crosslinked PVA with glutaraldehyde in the absence of acid. This reaction is done in 40^{o}C. An increase in glutaraldehyde concentration is known to create more branching of the polymer.[42]

Also in 2008, Chaouat et al. successfully fabricated crosslinked PVA with food grade crosslinker sodium trimetaphosphate in the presence of a strong base sodium hydroxide.[20] The exact mechanism of this reaction has not been studied; however, our group hypothesizes that sodium hydroxide might help to create oxygen radical that subsequently opens the trimetaphosphate ring, creating a phosphate bond that links two polymer chains together.

PVA has also been successfully used in many biomedical applications as summarized in Table 2 below.

Table 2. Biomedical applications of PVA hydrogel material

Crosslinking method	**Application**	**References**
Freeze-thaw	pH sensitive membranes for Theophylline drug delivery	Nugent et al.[38]
	Bioprosthetic heart valve stent	Wan et al.[44]
	Heart patch for basic-fibroblast growth factor delivery	Fathi et al.[45]
	Artificial knee meniscus for osteoarthrosis patient	Kobayashi et al.[46]
Electron beam	Soft contact lens	Yang et al.[47]
Chemical	Multilayered hydrogel film system for insulin delivery	Ding et al.[48]
	Vascular graft	Chaouat et al.[20] Cutiongco et al.[21-22]

Some of these works have reached pre-clinical study stage (in vivo implantation in animals) and one of the study reported minimal the inflammatory reaction minimal with moderate fibrous host

tissue response around the scaffold,[45] while the other did not observe any significant inflammatory reaction, indicating the biocompatibility of PVA.[46]

1.7 The current state of small diameter PVA vascular graft

The suitability of PVA for making a small diameter vascular graft is determined by its property. Firstly, PVA is non-toxic, non-immunogenic, non-carcinogenic, and highly biocompatible. PVA is highly hydrophilic and without any addition of biomolecules or any bulk/surface modifications, PVA is biologically inert. Therefore, it is non-platelet activating or non-thrombogenic as shown previously by our group with an in vitro study using platelet rich plasma incubation and scanning electron microscopy method to assess the platelet shape on PVA surface.[21] PVA flexibility can range from 0.7 MPa[49] to 46 GPa[50] depending on the crosslinking method and the degree of crosslinking between the polymer chains. The wide range of Young's modulus allows PVA to be made flexible enough to match the stiffness of native blood vessel. Study has also shown that PVA has decent burst pressure and suture retention strength to withstand pulsatile flow in vivo.[20]

A study of small diameter STMP crosslinked PVA vascular graft (2 mm diameter) was first published in 2008. The graft was made from crosslinked PVA film which was wrapped around a PTFE rod and was either glued or sutured to connect the two edges to create a tube.[20] The small diameter grafts were implanted in rat aorta with end-to-end anastomosis and maintained their patency after 1 day and 7 days of implant. Continuing from this study, our group fabricated PVA grafts with dip casting method and performed in vitro cell study of patterned PVA films as well as in vivo study of 2 mm diameter PVA grafts with surface topography in rat aorta. What we found from the in vitro cell study was that the attachment of endothelial cells on patterned PVA surfaces

with 2x2x2 μm gratings and 1.8 μm concave lenses topography was significantly improved compared to unpatterned PVA, although the endothelial monolayer can be achieved only on N_2 plasma treated PVA films after 6 days in culture. On these substrates also, the contact angle was measured and we observed that 2 μm gratings and 1.8 μm concave lenses has significantly higher contact angle compared to the unpatterned PVA control which means that the apparent surface wettability of these substrates have changed and resulted in an improved endothelialisation in vitro. Furthermore, the implanted grafts were implanted with end-to-end anastomosis for 20 days in the rat model. Both PVA grafts with 1.8 μm convex lenses topography and unpatterned surface were occluded, while 2 μm gratings, 2 μm pillars, and 1.8 μm concave lenses show partial graft patency after 20 days. In another in vivo study with a rabbit model, our group has also implanted submillimeter PVA grafts (0.9 to 1 mm diameter) with unpatterned surfaces at rabbit femoral artery and achieved 14- to 17-day patency rate of 67%.

1.8 Limitations of small diameter PVA grafts and hypotheses

Despite the excellent mechanical property tunability, PVA material requires surface modification to improve graft endothelialisation and, at the end of the day, graft patency. From the previous in vitro cell adhesion study, N_2 plasma modification seemed to improve endothelial cell attachment of PVA films.[23] However, to utilize this surface modification for a vascular graft, luminal plasma treatment is required instead. Mantovani et al. has previously shown a technique to plasma treat ePTFE graft lumen of 10 mm inner diameter with NH_3 plasma.[51] However, on small diameter grafts (≤ 6 mm diameter), the feasibility of this technique has never been tested before.

The implanted PVA grafts in rat and rabbit model were all sterilized with γ-radiation. However, there are more than one options to terminally sterilized a hydrogel material. Some studies have shown the effect of EtO and γ-radiation terminal sterilization on material and mechanical property of polymer other than chemically crosslinked PVA.[52-53] Because the sterilization step can create changes on the material, studying the effect of it on graft mechanical property and endothelialisation is important and has never been explored before.

Achieving 67% patency rate over 15-17 days of submillimeter PVA graft implantation in rabbit femoral artery is commendable. However, the implantation was done with end-to-end anastomoses as in other small diameter synthetic vascular graft studies; while end-to-side anastomosis is a more clinically relevant method. It was not known whether by changing the anastomoses method, graft endothelialisation will be affected given the change in hemodynamic and longer graft length; and furthermore if the graft can remain patent when the implant duration is increased to 28 to 30 days.

In this thesis, we hypothesize that in vitro and in vivo endothelialisation of small diameter PVA grafts can be enhanced by the luminal surface modification method and will not be affected by graft sterilization process. Specifically, we hypothesize that the effect of this plasma modification in combination with the microtopography would enhance endothelialisation further without invoking severe platelet activation reaction. We also speculate that γ-radiation minimally changes graft mechanical property and that it has minimum toxicity which could affect surface endothelialisation. Lastly, we hypothesize that PVA grafts will maintain its patency at 28 to 30 days of implant.

1.9 Research scope and thesis outline

The research focus of this thesis can be outlined into 3 main aims which correspond to chapter 2, 3, and 4 of this thesis:

(a) Aim 1: Luminal modification of small diameter PVA vascular graft

PVA hydrophilicity makes its surface unfavorable for cell attachment; while endothelialisation of a graft lumen can help to prevent thrombus and IH formation. Hence, surface modification of the PVA graft is necessary to improve endothelial cell attachment. Specifically, in vitro cell adhesion study with human umbilical vein endothelial cell line, EA.hy926 on the modified and unmodified PVA graft will be reported. This consists of surface characterization of the modified PVA surfaces, and quantification of cell number and endothelial cell gene and markers expression. In addition, platelet activation test result of the modified PVA graft will be reported as alteration of surface property (preferring cell attachment) could increase platelet activation level.

(b) Aim 2: Effect of terminal sterilisation on PVA graft and endothelialisation

Prior to implantation to an animal model, it is necessary to sterilize PVA grafts. An ideal sterilization method should maintain graft mechanical, physical, and chemical property while being effective in inactivating microorganism. The effect of two terminal sterilization method, EtO and γ-radiation will be investigated. Specifically, changes in mechanical and material properties will be reported. Mechanical properties include radial compliance, minimum bend radius, burst pressure, suture retention strength, and Young's modulus, while material property include FTIR spectra, crystallinity degree, XPS, and water contact angle. In addition, changes in endothelialisation of PVA and surface topography and contact angle will be reported.

(c) Aim 3: In vivo study of PVA vascular grafts

In vivo study using a relevant animal model is needed to prove graft safety, efficacy, and patency in order to better achieve a success in clinical trial. Rabbit is chosen as a suitable animal model to test our small diameter PVA vascular grafts. Specifically, successful PVA graft implantation in end-to-side configuration and patency rate assessment will be reported. Graft patency and endothelialisation will be assessed based on ultrasound flow measurement and histology. Preliminary observation of graft compliance correlation with IH formation will also be reported.

CHAPTER 2

Luminal modification of small diameter PVA vascular grafts

2.1 Introduction

The expression of cell adhesion molecules (CAM) on cells surfaces affects the ability of cells to interact with their surrounding environment. The higher expression of CAM creates larger contact area and affinity to a material surface. Given this fact, cell attachment and interaction with its surrounding is an active phenomenon, unlike the non-living colloidal system in general.[54] The non-specific binding due to Van der Waals forces may hence be superseded by the short range specific interaction called the ligand-receptor binding.[54] This specific interaction is highly dependent on spatial organization of the binding site at the receptor and the interaction is sequence specific.[55-56]

In particular, cells- material interaction is facilitated by cell membrane receptors called integrins which are collectively known as focal adhesion.[57] Each integrin has a specific ligand type which helps a cell to anchor onto material surface. The configuration of ligands on surface material can also promote other cell responses including cell migration,[58] cell alignment[59] and cell differentiation.[60] Therefore, the improvement of cell adhesion on a material surface can be achieved by providing ligands to the integrin which can be done through adding certain function groups (amine, amide, or carbonyl) on the biomaterial surface or through improving protein/ ligand immobilization on the material surface by hydrophobic interaction.

One of the well-recognized techniques to promote cell adhesion on a material surface is through plasma treatment. Plasma is an ionized gas consisting of free electrons and positive ions which make it highly conducting. The chemistry of plasma affects the type of functional group that is formed on the surface; this functional group facilitates the interaction between proteins and biomaterial surface. For example, silanol group (polar) is formed when treating polydimethyl siloxane (PDMS) with oxygen plasma,[61] while carboxyl, hydroxyl, vinyl and thiol functional

groups can be created by treating the material surface with CO_2, hydrogen, oxygen, hydrogen sulfide plasma, respectively. The H_2/N_2 plasma treatment has been known to have the capability to surface functionalize flat PVA film surface via the introduction of amide, carboxylic acid, and OH/NH function groups.[62] This result was confirmed through FTIR spectra which reveal the new peaks appearance at 1654 cm^{-1}, 1705 cm^{-1}, and 3200-3400 cm^{-1} respectively. The use of plasma treatment to modify a lumen of a tubular structure, however, has not been widely employed.

Mantovani et al. has successfully developed a luminal NH_3 plasma treatment system to treat ePTFE vascular graft of length 20-150 mm long and ID 10 mm wide.[51] With the similar set up, herein, the result of a more challenging NH_3 plasma modification for a small diameter vascular graft ($\leq$ 6 mm internal diameter (ID)) will be reported.

Alteration of apparent surface hydrophilicity can also be done through introducing microtopography on the graft luminal surface. However, due to the high aqueous content of PVA hydrogel, it is difficult to perform traditional lithography techniques to create micropatterns on PVA. Moreover, performing photolithography on hydrogel could result in the generation of cytotoxic photoinitiators.[63-64] Our group has previously reported that using a simple casting method and ultrasonication, we are able to pattern PVA graft lumen with good fidelity.[23] Herein, by employing the same fabrication method, two selected microtopographies which have been shown to improve endothelial cell attachment will be fabricated. These topographies are 2x2x2 μm gratings and 1.8 μm concave lenses. As any alteration in surface property can also change platelet response to the biomaterial surface, the modified small diameter PVA grafts will also be tested for platelet activation and fibrin deposition by using ex vivo shunt model as reported previously.[65]

In this chapter, we are looking into the effect of luminal NH_3 plasma treatment together with the selected microtopographies on the attachment of human umbilical vein endothelial cell line (EA.hy926) on the PVA small diameter vascular graft and on the platelet activation with ex vivo shunt model. We hypothesize that: (1) NH_3 plasma alone can enhance endothelial cell attachment on PVA surface, (2) combination of surface topography and plasma modification improves further endothelial cell attachment on PVA surface, and (3) plasma modification minimally affects platelet activation.

2.2 Materials and Methods

2.2.1 PVA graft fabrication

The steps for crosslinking PVA with sodium trimetaphosphate (STMP) is prepared according to Chaouat et al.[20] In brief, 10% (w/v) PVA (Aldrich, Mw 85,000-124,000, hydrolysis percentage 87-89%) was mixed with 15% (w/v) STMP (Aldrich) for 5-10 minutes until homogeneous solution is obtained. Afterwards, 30% (w/v) NaOH (Sigma-Aldrich) was added into stirring solution and the solution was mixed for another 5-10 minutes. The solution was then centrifuged to remove any bubbles.

A cylindrical rod coated with crosslinking PDMS (base : crosslinker = 10:1) (Dow Corning, Sylgard 184) was cured at 60^{o}C. The PDMS coated needle was air plasma treated (85W, 0.8 NL/h) for 80 seconds and was coated with layers of crosslinking PVA solution. Coated cylindrical rod was then kept in a cabinet with controlled temperature of 20^{o}C and controlled humidity of 70% for 3 days. Afterwards, PVA coated cylindrical mold can be rehydrated in deionized water and demolded from the mold (see Figure 1).

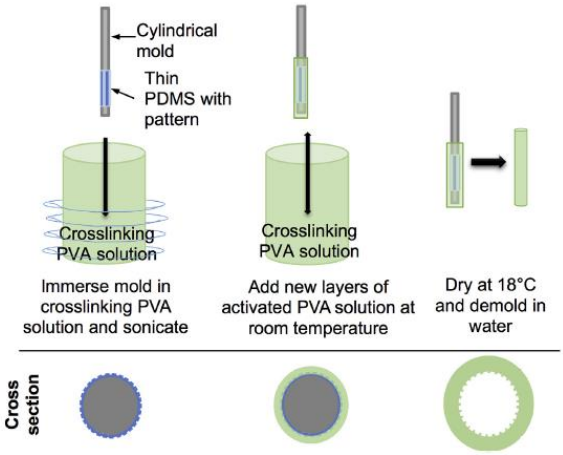

Figure 1. Schematic diagram of polyvinyl alcohol (PVA) graft fabrication with dip casting method, adapted from Cutiongco et al.[23] Reproduced with permission from Elsevier.

2.2.2 PVA film fabrication

Similar to the aforementioned method, 10% (w/v) PVA was mixed with 15% (w/v) STMP for 5-10 minutes until homogeneous solution is obtained. Afterwards, 30% (w/v) NaOH was added into stirring solution and the solution was mixed for another 5-10 minutes. The solution was then centrifuged to remove any bubbles and was poured into dishes. The dishes were kept in a cabinet with controlled temperature of 20^{o}C and controlled humidity of 70% until the PVA film is completely dried. Afterwards, PVA film can be rehydrated in deionized water and demolded from the dishes.

2.2.3 Patterned PVA graft fabrication

The preparation of crosslinking PVA solution is as mentioned above. A thin layer of micropatterned PDMS was made by spin coating of 2g of crosslinking PDMS (base : crosslinker = 5:1) on a patterned PDMS mold at 1500 rpm for 15 seconds. Afterwards, the thin PDMS layer was rolled around the cylindrical rod and was air plasma treated as before. The rod was kept in crosslinking PVA solution and was sonicated for at least 90 minutes at 49 kHz. The cylindrical

rod was then coated with layers of crosslinking PVA and it was kept in a cabinet as before. The rehydration of the PVA patterned tubes was done in 10x Phosphate buffered saline (PBS) (Fisher Scientific) followed by 1x PBS and deionized water.

2.2.4 Patterned PVA film fabrication

The preparation of crosslinking PVA solution is as mentioned above. Crosslinking PVA solution was poured on a dish with PDMS patterned mold. The dish was centrifuged at 600 rpm for 1.5 hours and was kept in a cabinet with controlled temperature and humidity as before until PVA film was fully dried. The rehydration of patterned PVA film was done in 10x PBS followed by 1x PBS and deionized water.

2.2.5 Scanning electron microscopy

PVA was dehydrated and coated with gold nanoparticle. Scanning electron microscope images were taken with a high-resolution field-emission scanning electron microscope (Zeiss 1550, Carl Zeiss AG, Oberkochen, Germany) at accelerated voltage of 7 keV.

2.2.6 Luminal NH_3 Plasma Treatment

Luminal NH_3 plasma treatment with RFGD treatment system was performed as previously described.[51] In brief, a dehydrated PVA graft was inserted into a cylindrical Pyrex glass tube. Three capacitively coupled copper electrodes were located at the middle section of the tube for plasma generation. After pressure of less than $5x10^{-5}$ Torr was reached, high purity NH_3 gas was introduced into the chamber from the inlet which was 5 cm below the upper end of the tube. The NH_3 plasma ignition was initiated by a radio-frequency generator thereafter and modified the luminal surface of the PVA graft.

2.2.7 X-ray photoelectron spectroscopy (XPS) measurement

The chemical composition of the surface was investigated by XPS PHI 5600-ci spectrometer (Physical Electronics, Eden Prairie, MN). The main XPS chamber was maintained at a base pressure of < $8x10^{-9}$ Torr. An achromatic aluminium X-ray source (1486.6 eV) was used at 300W with a neutralizer to record the survey spectra, and a standard magnesium X-ray source (1253.6 eV eV) was used to record high resolution spectra of C1s, without charge neutralization. The detection angle was set at 45^{o} with respect to the normal of the surface and the analyzed area was 0.125 mm^2. Measurement was done at 11 equidistant positions along a 5.5 cm long dehydrated PVA graft.

2.2.8 Water contact angle measurement

Water contact angle was measured on sterilized and non-sterilized PVA films using an in-house built instrument. PVA films were hydrated during the test and its surface was dabbed dry prior to test. The water volume used for measurement is 3 µl and images were captured within 10 seconds after the water drop was on the film surface.

2.2.9 EA.hy926 adhesion study on PVA luminal surfaces

Unpatterned (UP) PVA tube and two other types of topographies were used in this study: 2 µm gratings (2µG), and 1.8 µm concave lenses (CCL) tubes. Plasma treated tubes were indicated with a letter P behind the abbreviation, i.e. UPP, 2 µGP, CCLP for plasma treated unpatterned, 2 µm gratings, and 1.8 µm concave lenses tubes, respectively. PVA tube was cut open longitudinally and sterilized with UV for 20 minutes, followed by incubation with 10% Penicillin/Streptomycin (Gibco) and 1% Amphotericin-B (VWR). PVA was then fixed in a 24-well plate with autoclaved silastic tubings using sterilized forceps and was rinsed thoroughly with 1x PBS. Afterwards, PVA was incubated with fetal bovine serum (FBS) (Gibco) followed by centrifugation at 1000 rpm for

30 minutes. PVA can be kept in 2-8ºC fridge overnight or in 37ºC incubator for 30 minutes prior to cell seeding.

EA.hy926 (ATCC) cell passage number used in this study is passage number 7. EA.hy926 culture was done according to ATCC protocol. Confluent cells were passaged with 0.05% Trypsin/EDTA (Gibco) and were seeded on the PVA at seeding density 50,000 cells/cm^2. The well plate was then spun down at 100xg for 10 minutes to bring the cells down closer to the PVA substrate. Cells were cultured for 13 days before performing subsequent cell analysis (section 2.2.8 to 2.2.10).

2.2.10 Cell number quantification

Quantifications of cell number on PVA samples were done with CyQUANT® Cell Proliferation Assay Kit (Invitrogen) as per manufacturer protocol. In brief, after being in culture for 13 days, cells were passaged and collected into microcentrifuge tubes. Cell suspension was then spun down at 1500 rpm for 5 minutes and followed by washing of the cell pellet in 1xPBS to minimize the interference of phenol red to the intensity reading. Fluorescence measurement was done at 530 nm wavelength and the measured values were translated into cell number by using a standard curve equation: $n = 4.086 * I + 151.15$, where n is the cell number and I is the fluorescence intensity. R^2 value of this equation is 0.9976

2.2.11 Gene expression quantification

Quantifications of platelet endothelial cell adhesion molecule 1 (PECAM1) and endothelial nitric oxide synthase (NOS3) gene expression were done with RT-qPCR and normalized to the 18s ribosomal RNA (18s rRNA) as the endogenous control. Forward and reverse primer sequences are as published before[66] for PECAM1 (forward: 5'-AACAGTGTTGACATGAAGAGCC-3',

reverse: 5'-TGTAAAACAGCACGTCATCCT-3'), NOS3 (forward: 5'-TGATGGCGAAGCGAGTGAAG-3', reverse: 5'-ACTCATCCATACACAGGACCC-3'), and 18s rRNA (forward: 5'-GGCCCTGTAATTGGAATGAGTC-3', reverse: 5'-CCAAGATCCAACTACGAGCTT-3') (Sigma, Easy™ Oligos). RNA isolation was performed with RNeasy® Mini Kit (Qiagen) according to the manufacturer protocol. cDNA strand was then synthesized using SuperScript® III First-Strand Synthesis System (Invitrogen) according to the manufacturer protocol. Lastly, amplification of gene specific region was done using SsoFast™ EvaGreen® Supermix with Low Rox (Bio-Rad) also according to the manufacturer protocol. Measurements were run in triplicates for each of the experimental groups.

2.2.12 Cell immunofluorescence staining

To prevent the disruption of cell-cell junction, culture was washed with DPBS buffer (1x) (Gibco) prior to fixation with 4% paraformaldehyde (PFA) (Sigma Aldrich) for 15 minutes. Cells were permeabilized by incubation with 0.05% Triton X-100 (Sigma) and 50 nM glycine (Aldrich) for 15-20 minutes. Cell nuclei and F-actin staining was done with DAPI (1:5000) and Phalloidin (1:500) (Invitrogen) incubation for 30 minutes respectively.

2.2.13 Cell image acquisition and analysis

Cells were imaged using Zeiss immunofluorescence microscope at 20x magnification. Images were taken at random positions on the PVA surface and the most representative images were selected for brightness and contrast adjustment using ImageJ software.

2.2.14 Baboon ex vivo shunt study

All baboons (Papio anubis) were housed and taken care of by Oregon National Primate Research Center (ONPRC) according to "Guide to the Care and Use of Laboratory Animals" and is approved by ONPRC Institutional Animal Care and Use Committee.

The ex vivo shunt study was done by our collaborator, Dr. Deirdre Anderson at OHSU/ONPRC. Prior to experiment, baboon platelets were labeled with 111-Indium and homologous fibrinogen was labeled with 125-Iodine. Baboon femoral artery and vein were accessed and extended with silicon tubing where the PVA graft was attached to for 60 minutes without anticoagulant or anti-platelet administration. Afterwards, graft was flushed and fixed with 10% PFA for platelet and fibrinogen quantification.

2.2.15 Statistical analysis

Statistical comparisons between experimental groups were done using one-way ANOVA and Tukey's post-hoc analysis unless otherwise stated in the figure legend. Data were presented as mean ± standard error. * denotes statistical significance with p-value of less than 0.05, ** p-value ≤ 0.01, *** p-value ≤ 0.001, and **** p-value ≤ 0.0001, all is with 95% confidence level. Sample size will be reported in the individual figure legend.

2.3 Results

2.3.1 Micro patterns on PVA luminal surface show good fidelity

PVA tubes with 2 μm gratings and 1.8 μm concave lenses topography used for the in vitro cell adhesion study were successfully fabricated with good fidelity as shown in Figure 2.

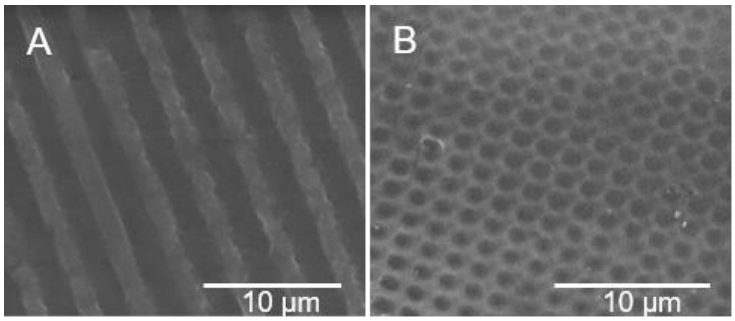

Figure 2. SEM images of PVA luminal surface patterned with (A) 2 µm gratings and (B) 1.8 µm concave lenses topography.

2.3.2 Increase in nitrogen percentage on plasma treated PVA luminal surface

An increase in nitrogen percentage on the plasma treated PVA surface was observed, indicating successful introduction of N species on the PVA surface (Figure 3). The %N along the plasma treated PVA luminal surface, measured at 11 equidistant positions, averaged at 9.4% while on PVA luminal surface without plasma, there was no nitrogen element detected.

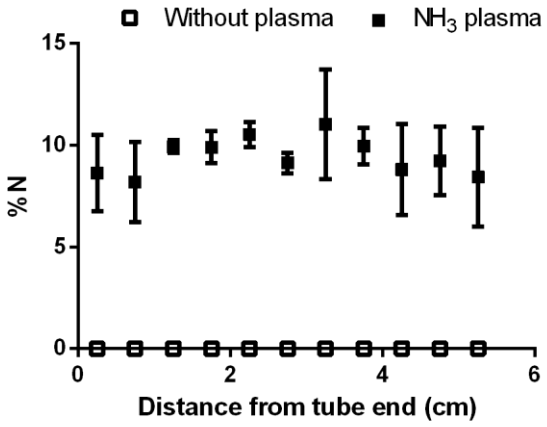

Figure 3. XPS measurement of PVA luminal surface without plasma (n=3) and after NH_3 plasma treatment (n=3) measured at 11 equidistant positions along the 5.5 cm-long tube. All data were presented as mean ± standard error.

2.3.3 Water contact angle measurement reveals higher hydrophobicity on plasma treated PVA surfaces

Water contact angle of the all plasma treated PVA surface for all topographies (unpatterned, 2 μm gratings, 1.8 μm concave lenses) was found to be higher than the untreated PVA group (Table 3). Contact angle on untreated 1.8 μm concave lenses topography was unable to be measured as it is very close to 0^o. Statistical significance was found between the contact angle of plasma treated unpatterned PVA surfaces and plasma treated 1.8 μm concave lenses PVA surfaces ($p \leq 0.05$, n=6).

Table 3. Water contact angle measurement of PVA surface without plasma and with NH_3 plasma. All data were presented as mean ± standard error, n=6.

	Unpatterned	2 μm gratings	1.8 μm concave lenses
Without plasma	18.8 ± 1.4^o	20.5 ± 3.2^o	Cannot be measured[(a)]
NH_3 plasma	30.5 ± 6.0^o	26.3 ± 5.2^o	14.5 ± 2.0^o

(a) Contact angle was close to 0^o

2.3.2 Improvement of cell adhesion on modified PVA graft luminal surface

Among the three different topographical surfaces, 2 μm gratings topography consistently supported better endothelial cell attachment (Figure 4B, E). The best cell attachment was, however, found on the NH_3 plasma treated 2 μm gratings PVA tube, forming an endothelial monolayer on the PVA luminal surface (Figure 4E). On all topographies, the cells morphology is mostly rounded with a better cell alignment observed on the untreated 2 μm gratings rather than the plasma treated 2 μm gratings. Cells on 1.8 μm concave lenses, with and without NH_3 plasma, show the second-best attachment with random orientation, followed by the unpatterned PVA tube. The cell number quantification (Figure 4H) shows that NH_3 luminal plasma treatment improves the endothelial cell

attachment on the PVA; however, the differences between attachment on PVA surfaces are not statistically significant (n=3).

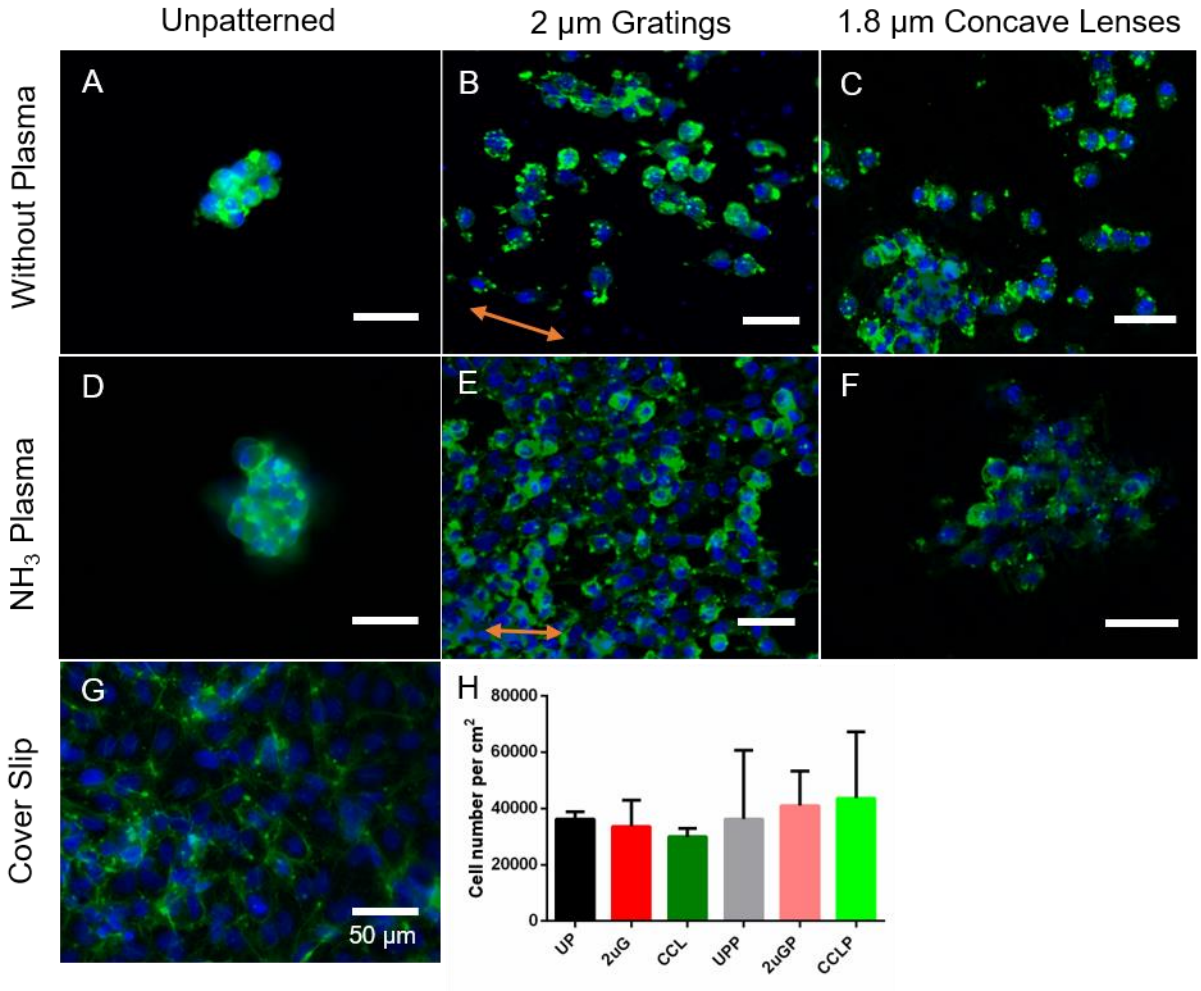

Figure 4. EA.hy926 cell attachment on PVA surfaces without plasma treatment (A-C) and with NH3 plasma treatment (D-F) on unpatterned (A, D), 2 µm gratings (B, E), and 1.8 µm concave lenses topography (C, F) after 13 days in culture. Orange arrows indicate the gratings direction of 2 µm gratings topography. Endothelial monolayer formation was observed on plasma treated 2 µm gratings topography (E) and on cover slip control (G). Nuclei are shown in blue and F-actins are shown in green. Scale bars in all figures are 50 µm. (H) Cell number quantification on PVA surfaces with different luminal modifications (UP = unpatterned, 2uG = 2 µm gratings, CCL = 1.8

μm concave lenses, UPP = unpatterned with plasma, 2uG = 2 μm gratings with plasma, CCLP = 1.8 μm concave lenses with plasma) indicates higher cell number on plasma treated PVA surfaces. However, no statistical significance was found (n=3).

2.3.3 PECAM1 and NOS3 genes were upregulated and downregulated on PVA surfaces without and with plasma modification, respectively

PECAM1 and NOS3 genes were selected among other endothelial cell genes because the protein expression of PECAM1 was known to involve in cell-cell junctions, whereas the protein expression of NOS3 was known to involve in important endothelial functions of vasodilation, platelet inhibition, and anti-thrombogenic agent. The upregulation and downregulation of both PECAM1 and NOS3 genes show similar trend (Figure 5). Both genes are upregulated in cells that were grown on 2 μm gratings and 1.8 μm concave lenses topography without NH_3 plasma modification. Interestingly, the expression of PECAM1 and NOS3 genes were both downregulated in all plasma treated surfaces. Significant PECAM1 gene downregulation was especially observed on the plasma treated 1.8 μm concave lenses topography; the difference of PECAM1 expression in 1.8 μm concave lenses topography with and without plasma treatment was highly significant ($p \leq 0.001$, n=3).

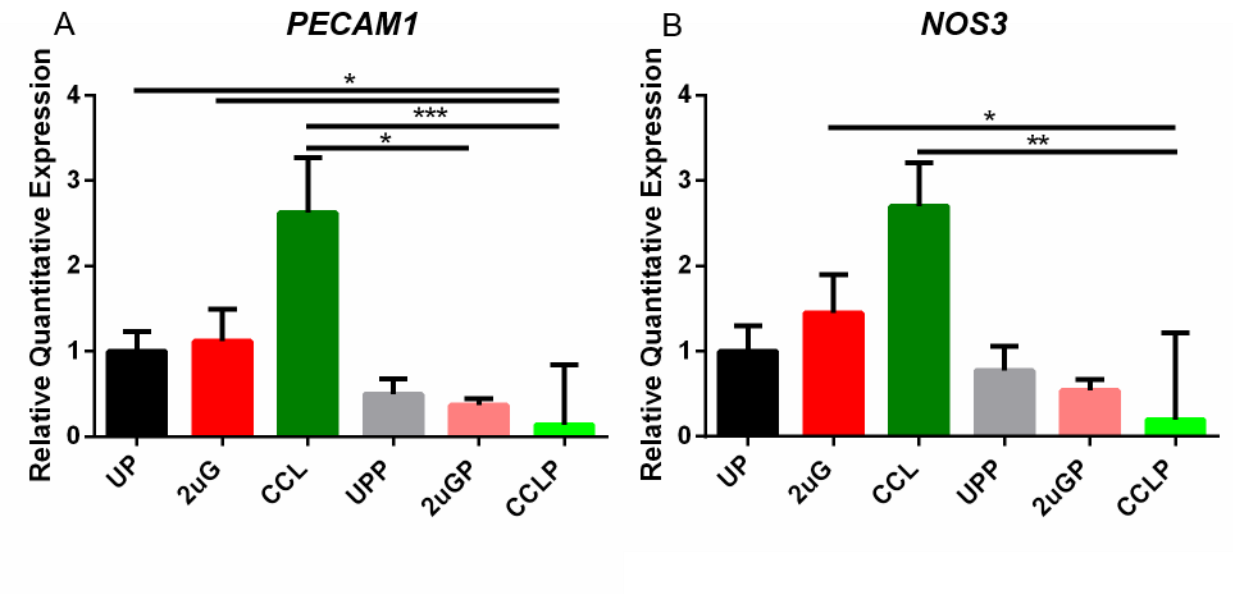

Figure 5. Relative quantitative expression of endothelial cell genes: (A) PECAM1 and (B) NOS3 to the respective expression on unpatterned PVA substrate (UP). PECAM1 gene upregulation on 1.8 µm concave lenses topography without plasma was 1.6-fold higher than the unpatterned PVA substrate, while NOS3 was 1.7-fold higher. In general, both genes were upregulated on untreated PVA surfaces, while they were downregulated on NH3 plasma treated surfaces. * denotes statistical significance with p-value of less than 0.05, ** p-value ≤ 0.01, and *** p-value ≤ 0.001, n=3.

2.3.4 Ex vivo shunt studies show higher platelet and fibrin accumulation on plasma treated concave lenses PVA tubes

Platelet accumulation was measured every minute over one-hour duration of study (Figure 6). The highest platelet accumulation occurred on the collagen coated tube which serves as a positive control. Interestingly, plasma treated PVA tube with 1.8 µm concave lenses topography shows high platelet accumulation with higher mean compares to ePTFE graft. However, there difference in mean was not statistically significant. Platelet accumulation on the plasma treated 1.8

μm concave lenses topography was, however, found to be significantly higher than the accumulation on plasma treated 2 μm gratings topography ($p \leq 0.05$, n=6). Moreover, the unpatterned plasma treated PVA tube has low platelet accumulation and was comparable to the untreated PVA tubes with or without patterns.

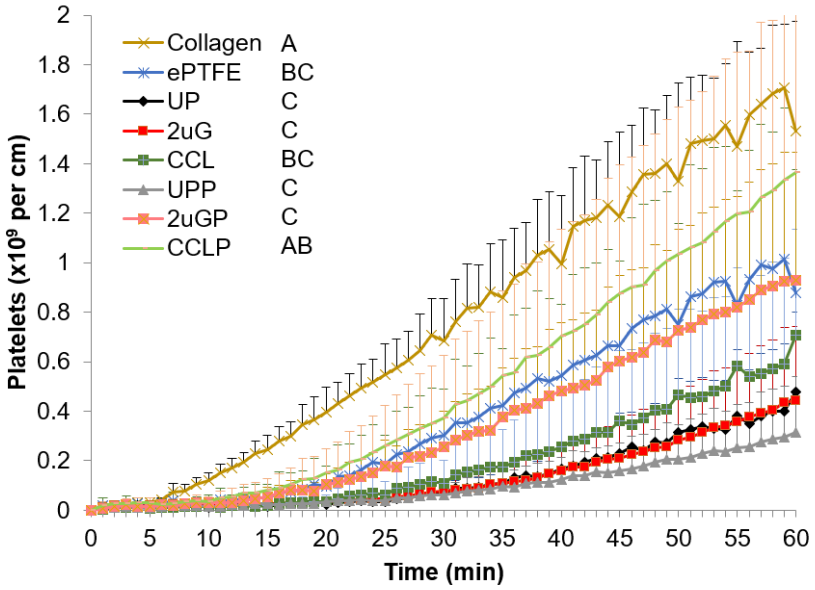

Figure 6. Platelet accumulation measurement with *ex vivo* shunt model. Statistical analysis performed with repeated measures ANOVA on 5 minutes timepoint data. Experimental groups are categorized into A, B, and C based on their statistical similarities. P-value between different statistical group is ≤ 0.05, n=6.

This result agrees with the fibrin accumulation data which was collected after complete decay of Indium-111, where plasma treated 1.8 μm concave lenses tube show the highest fibrin accumulation and was comparable to collagen coated positive control (Figure 7). On the PVA samples, both plasma-treated and non-plasma treated tube follow the same trend whereby the 1.8 μm concave lenses tube shows the highest fibrin accumulation, followed by 2 μm gratings and the

unpatterned tubes. The difference in fibrin accumulation between unpatterned tubes (with or without NH_3 plasma) and the plasma treated 1.8 µm concave lenses tubes was statistically significant ($p \leq 0.05$, n=6).

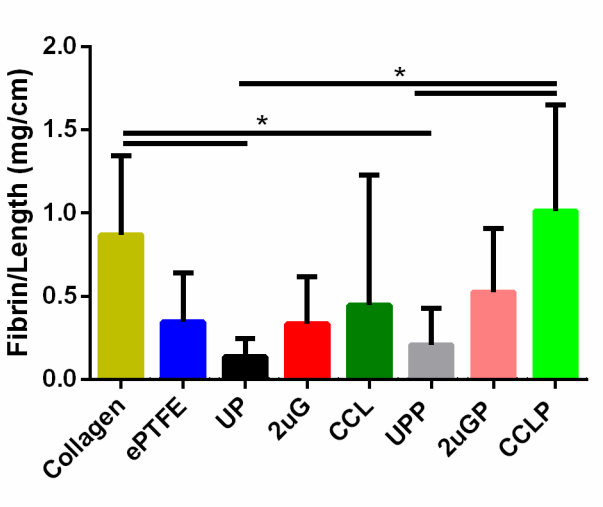

Figure 7. Normalized fibrin accumulation amount at the end of ex vivo shunt runs. Statistical analysis was performed with 2-way ANOVA. * denotes statistical significance with p-value ≤ 0.05, n=6.

2.4 Discussions

In this study, PVA tube luminal surface was treated with NH_3 plasma which introduces N species to the PVA surface and facilitates specific interaction between PVA surface and endothelial CAMs through receptor-ligand binding. Moreover, the presence of surface topography is useful in altering PVA apparent hydrophilicity which in turn promote hydrophobic interaction with extracellular matrix proteins present in the serum (from initial sample incubation) as well as in culture media. The modification of –OH function group as well as alteration in hydrophilicity act synergistically to promote endothelialisation of the PVA material. Moreover, topography isotropicity as in the case of 2 µm gratings topography helps to improve cell elongation and

alignment by providing guidance to the focal adhesions. In the case of adherent cell type like endothelial cells, good cell anchorage and spreading allows F-actin stress fibers to form and help in the subsequent cell functions.[67]

To detect the presence of N species on the PVA surface after plasma modification, XPS measurement was performed. An increase in %N element on the plasma treated PVA surface was observed, while on the surface without plasma, there was no %N detected. The change in surface property was further characterized by measuring water contact angle of the PVA surface. As observed previously,[23] the presence of N species on PVA surface create a more hydrophobic surface property; the trend is consistent across different topographies. Meanwhile, the presence of topography increases exposed surface area to plasma modification. Better cell attachment on 2 μm gratings and 1.8 μm concave lenses topography compares to the unpatterned PVA group was, therefore, expected and can be observed from Figure 4. Interestingly, cell alignment was observed more clearly on 2 μm gratings topography without plasma which suggests that on this substrate, cells were given more space to sense their underlying topography before they come in contact with one another.

PECAM1 gene involves in the expression of CD31 adhesion molecule at the endothelial cell-cell junction. Meanwhile, NOS3 gene is one of the phenotypic genes in endothelial cells and it involves in various EC functions.[66] Endothelial nitric oxide synthase (eNOS), an endothelial marker expression of NOS3 gene, is responsible in the production of nitric oxide (NO) which is a vasodilator,[11] a platelet function inhibitor, and an anti-thrombogenic agent.[68] The expressions of PECAM1 and NOS3 gene were measured with RT-qPCR and all groups were normalized to unpatterned PVA without plasma group. Both genes were observed to be upregulated on the non-plasma treated PVA surfaces with both gratings and micro lenses topographies; however, it is

interesting to see that on plasma treated surfaces, the expression of these genes were both downregulated with plasma treated 1.8 μm lenses topography showing the lowest gene expression. The higher expression of PECAM1 gene could mean a higher expression of CD31 proteins on the cell surface and a better contact between cells. In the case of the non-plasma treated PVA surfaces, the upregulation of PECAM1 could be caused by cell aggregate formation as often found from the qualitative observation of EA.hy926 cells on non-plasma treated PVA surfaces. More experiment will be needed to confirm this finding and to better compare between samples with adherent monolayer. Furthermore, it is possible to validate this finding by immunofluorescence staining to check protein expressions; this will be part of our future works.

Surface modification to favor cell attachment can promote endothelial cell lining in the graft lumen which could prevent thrombosis and improve graft patency. However, in the *in vivo* environment, platelet can also attach and be activated to a bioactive surface before endothelial cell layer is established. Platelet initiates blood clotting process by aggregating with one another at its active conformation. Moreover, fibrin which comes from a different coagulation cascade helps to strengthen the structure by attaching to the clot, forming a mesh-like structure. The result of baboon *ex vivo* shunt study shows an increase in the number of activated platelet over the 1-hour study. Interestingly, platelet activation on the plasma treated 1.8 μm concave lenses topography were significantly higher than the other PVA experimental groups except for the 1.8 μm concave lenses topography without plasma. Fibrin accumulation result shows similar trend, but statistical significance was found between plasma treated 1.8 μm concave lenses topography tube and the unpatterned PVA tubes with and without plasma. Meanwhile, the 2 μm gratings topography show similar platelet and fibrin accumulation to the unpatterned samples with or without plasma treatment. This result is consistent with our previous finding with in vitro LDH assay on untreated

PVA films with gratings and lenses topography.[21] We speculate that 1.8 μm lenses topography is a more favorable surface for platelet activation due to its anisotropicity and small gap between lenses. The degree of platelet activations of the other PVA groups were still significantly lower than the collagen coated glass positive control but show similar or lower platelet and fibrin accumulation compares to the ePTFE grafts.

2.5 Conclusions

This study has shown the potential of NH_3 luminal plasma treatment to improve endothelialisation of PVA graft, particularly on 2 μm gratings topography. The PECAM1 and NOS3 expression were downregulated on the plasma treated 1.8 μm concave lenses topography while the accumulation of activated platelet and fibrin were found to be the highest on this substrate. Meanwhile, on 2 μm gratings, the platelet and fibrin accumulation were moderate or low. Hence, we conclude that NH_3 plasma treated 2 μm gratings topography surface is ideal to promote PVA graft endothelialisation without invoking rapid blood coagulation cascade.

CHAPTER 3

Effect of Terminal Sterilization on PVA Graft and Endothelialisation

3.1 Introduction

Sterilization is a way to inactivate microorganism such as fungi, spores, and bacteria, and biological agents such as enveloped and non-enveloped viruses. An implant that is poorly sterilized could result in infectious agent build up and can cause the implant recipient to adopt diseases.

US Food Drugs and Administration (FDA) requires terminal sterilization step to be performed before a medical device can be implanted in a human body; only when terminal sterilization is not feasible, aseptic manufacturing technique is required to be performed. A few terminal sterilization methods that are FDA approved include steam, dry heat, ethylene oxide (EtO), radiation (γ-radiation or electron beam/E-beam). Each of the sterilization methods has its own advantages and disadvantages. Table 3 shows the microorganism inactivation ability of each of the terminal sterilization methods, adapted from Dai et al.[52]

Table 4. Microorganism inactivation ability of the FDA approved sterilization methods, adapted from Dai et al.[47]

Sterilization method	Inactivation level	Mycobacteria	Vegetative bacteria	Bacteria spores	Nonenveloped virus	Enveloped virus	Prions	Fungal
Heat-based	High	√	√	√	√	√	√	√
EtO	High	√	√	√	√	√	√	√
Gamma	High	√	√	√	√	√		√
E-beam	High	√	√	√	√	√		√

Both steam and dry heat are heat-based sterilization method with good penetrability. In particular, steam heat destructs replication components of a microorganism, while dry heat eliminates microorganisms through direct heat and oxidation reaction.[52] However, both of the sterilization methods can cause structural changes and degradation of thermosensitive polymer.[69-70] EtO sterilization effectively supresses metabolism and division of a microorganism or biological agents through irreversible alkylation of cellular components.[52, 71] However, studies have shown that EtO can accelerate polymer degradation and create toxic residual on the implant surface.[53, 72-73] Additionally, EtO was also found to increase crystallinity of poly(lactic acid) fiber scaffold and reduce the overall scaffold size.[70] Gamma and electron beam radiation methods offer a promising hydrogel sterilizing capability in that they sterilize at a relatively lower temperature and in a shorter duration. Also, these radiation methods are known to have high penetration, an ability to break down DNA and RNA and to create reactive oxygen species (ROS) that damages cellular components.[52, 74-75] However, some known drawbacks of the radiation method are that at the recommended dose of 25 kGy, radiation can cause scission of polymer chain which may lead to softening of polymer mechanical property as well as crosslinking reaction.[70, 76-77]

An ideal sterilization method should maintain graft mechanical, physical, and chemical property while being effective to inactivate microorganism. To our knowledge, terminal sterilization effect on STMP crosslinked PVA has not been investigated before. In this chapter, the effect of EtO and γ-radiation to PVA mechanical property, surface chemistry and topography, as well as crystallinity will be reported. We hypothesize terminal sterilization could affect the mechanical and chemical properties of PVA graft by changing the crystallinity.

3.2 Materials and Methods

3.2.1 PVA vascular graft and film fabrication

PVA graft and film fabrication and patterning were performed as explained in section 2.2.1 and 2.2.2. Two-millimeter diameter PVA grafts with different wall thickness were used in the sterilization study: PVA_a (0.27 ± 0.05 mm) and PVA_b (0.61 ± 0.06 mm) (see Figure 8).

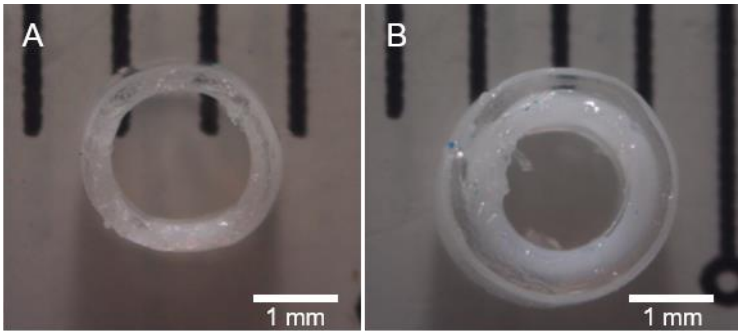

Figure 8. Cross-sectional view of (A) PVA tubular graft of internal diameter (ID) of 2mm, with 2 different wall thickness. PVA_a with thinner wall with mean thickness of 0.27mm (0.27 ± 0.05 mm, n=3) and (B) PVA_b with thicker wall with a mean thickness of 0.61mm (0.61 ± 0.06 mm, n=3).

3.2.2 Sterilization treatment

Gamma-radiation with dosage of 25 kGy was generated by an annular Co-60 source. Irradiation service was provided by Evans laboratory at the University of Toronto.

Sterilization with ethylene oxide (EtO) gas was performed with the following process parameters: preconditioning phase for 90 minutes at 55^{o}C and minimum relative humidity (RH) of 70% at puncture, EtO exposure phase for 60 minutes with EtO concentration of 759 mg/L at pressure range 400-650 mbar, and aeration phase for 12 hours at 55^{o}C. Sterilization was performed at Oregon National Primate Research Center (ONPRC).

3.2.3 Mechanical characterization

3.2.3.1 Compliance test

For testing of the vascular graft mechanical compliance, a vascular graft of length 3 cm with diameter of 2 mm respectively was exposed to intramural pressure 80 mmHg and 120 mmHg. The diameter change was captured with stereo microscope with 0.8X magnification and was measured using ImageJ software. Compliance was then calculated with the formula: $\%C_{rad} = \frac{d_{120}-d_{80}}{d_{80}} \times 100\%$ and compliance unit of %/40 mmHg.

3.2.3.2 Uniaxial tensile test

Tests were carried out with Universal Mechanical Tester (UMT), 100-kg load cell, cross head speed 10 mm/min on a hydrated PVA graft. Gauge length was 1.8 to 2.0 cm. Prior to testing, both graft ends were dehydrated to give a better grip; the middle section (2.0 to 2.2 cm long) was in hydrated condition when tested.

3.2.3.3 Bend radius test

Tests were carried out using series of circles with diameter increment of 1 cm. Graft was wrapped around the circles until it reaches the minimum circle radius just before it kinked. The graft aspect ratio was 15:1 (length: diameter).

3.2.3.4 Burst pressure test

A close-ended graft was exposed to increasing intramural pressure through slow release of N_2 gas until it reached the maximum pressure it can withstand. Pressure was measured in psi and converted into mmHg. (1 psi = 51.71 mmHg)

3.2.3.5 Suture retention test

One throw of polyamide 6 suture (Ethicon, size 8-0 and 6-0 for PVA_a and PVA_b respectively) was used. Suture initial position was 3 mm away from the graft end and was tied onto a variable load which was increased continually until the graft was ripped. The weight of load at the rip was taken as suture retention strength of graft.

3.2.4 Surface and chemical modification

3.2.4.1 Fourier-transform Infrared Spectroscopy (FTIR)

FTIR was done using Bruker Tensor 27 with wavenumber ranges from 500-4000 cm^{-1}.

3.2.4.2 Scanning Electron Microscopy

PVA was dehydrated and coated with gold nanoparticle. Scanning electron microscope images were taken with a high-resolution field-emission scanning electron microscope (Zeiss 1550, Carl Zeiss AG, Oberkochen, Germany) at accelerated voltage of 7 keV.

3.2.4.3 Differential Scanning Calorimetry (DSC)

DSC was performed using DSC Q2000 (TA Instruments). Heating-cooling cycle was performed from 30^oC-260^oC with ramp 10^oC/min using hermatic aluminum pan as reference. Heat of fusion was calculated from the second cooling cycle.

3.2.4.4 X-ray photoelectron spectroscopy (XPS)

XPS measurement was performed using unmonochromated Al Kα 1486.6 eV, Thermo VG Scientific ESCALab 250 microprobe. The analytical chamber pressure was maintained at $2x10^{-9}$ mbar during measurement.

3.2.4.4 Water contact angle measurement

Water contact angle was measured on sterilized and non-sterilized PVA films using an in-house built instrument. PVA films were hydrated during the test and its surface was dabbed dry prior to test. The water volume used for measurement is 3 µl and images were captured within 10 seconds after the water drop was on the film surface.

3.2.5 Cellular characterization

3.2.5.1 EA.hy926 cell seeding on sterilized (γ-irradiated) and non-sterilized PVA films

Unpatterned (UP) PVA films and PVA films with 2 µm gratings topography (2uG) were cut in the size of a 24-well plate and were sent in a hydrated state for γ-radiation treatment. The films were then sterilized with UV for 20 minutes, followed by incubation with 10% Penicillin/Streptomycin and 1% Amphotericin-B for 1 hour at 37^{o}C. PVA was then fixed in a 24-well plate with autoclaved silastic tubings using sterilized forceps and was rinsed thoroughly with 1x PBS. Afterwards, PVA was incubated with fetal bovine serum (FBS) followed by centrifugation at 1000 rpm for 30 minutes. PVA can be kept in 2-8^{o}C fridge overnight or in 37^{o}C incubator for 30 minutes prior to cell seeding.

EA.hy926 (ATCC) cell passage number used in this study is passage number 8. EA.hy926 culture was done according to ATCC protocol. Confluent cells were passaged with 0.05% Trypsin/EDTA and were seeded on the PVA at seeding density 50,000 cells/cm^2. The well plate was then spun down at 100xg for 10 minutes to bring the cells down closer to the PVA substrate. Cells were cultured for 13 days before performing subsequent cell analysis (section 3.2.5.1 and 3.2.5.2).

3.2.5.1 Cytotoxicity qualitative assessment

For qualitative assessment of the toxicity of γ-irradiated PVA, cells were stained with LIVE/DEAD™ Cell Imaging Kit (Invitrogen) according to the manufacturer protocol. Prior to adding dyes, cell culture media was replaced with HEPES-BSS buffer (Lonza). Culture was incubated for 15 minutes at 37°C and washed twice with HEPES-BSS buffer prior to imaging.

3.2.5.2 Cell number quantification

Quantification of cell number on PVA samples was done with CyQUANT® Cell Proliferation Assay Kit as per manufacturer protocol as mentioned in section 2.2.8. In brief, after being in culture for 13 days, cells were passaged and collected into microcentrifuge tubes. Cell suspension was then spun down at 1500 rpm for 5 minutes and followed by washing of the cell pellet in 1xPBS to minimize the interference of phenol red to the intensity reading. Fluorescence measurement was done at 530 nm wavelength and the measured values were translated into cell number by using a standard curve equation: $n = 3.828 * I + 769.31$, where n is the cell number and I is the fluorescence intensity. R^2 value of this equation is 0.8727.

3.2.6 Statistical analysis

Statistical comparisons between experimental group were done using one-way ANOVA and Tukey's post-hoc analysis. Data were presented as mean ± standard error. * denotes statistical significance with p-value of less than 0.05, ** p-value ≤ 0.01, *** p-value ≤ 0.001, **** p-value ≤ 0.0001, with 95% confidence level. Sample size will be reported in the individual figure legend.

3.3 Results

3.3.1 PVA graft opacity changes after EtO sterilization

The opacity of PVA grafts appeared to be more translucent after EtO treatment; this change was more clearly observed in PVA_a group rather than PVA_b group. However, this phenomenon was consistently observed in all EtO sterilized PVA grafts (see Figure 9).

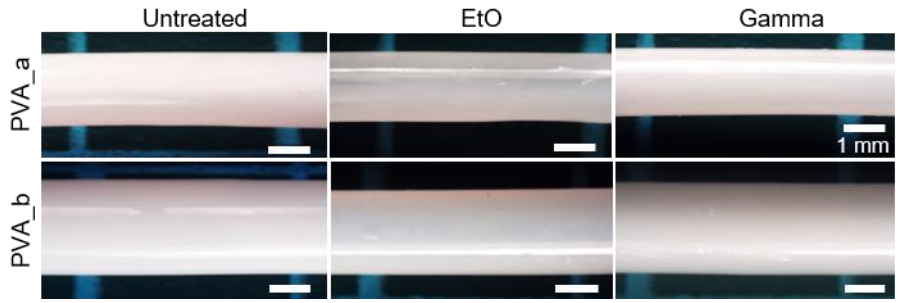

Figure 9. EtO sterilized PVA grafts were more translucent than untreated or gamma irradiated groups. This trend was consistently observed with PVA_b being less translucent than PVA_a group given the thicker graft wall thickness.

3.3.2 PVA mechanical properties change more drastically after EtO sterilization compares to γ-radiation

Graft compliance of EtO sterilized PVA significantly decreased as compared to untreated PVA control group ($p \leq 0.0001$ and $p \leq 0.05$ for PVA_a and PVA_b group respectively, n=4); while graft compliance of γ-irradiated PVA grafts significantly increased as compared to untreated PVA control group ($p \leq 0.0001$, n=4 for both PVA_a and PVA_b group, see Figure 10 A, B). The Young's modulus of PVA_a and PVA_b also confirms the observation for PVA graft compliance whereby EtO sterilized PVA_a and PVA_b have higher Young's modulus compares to the control untreated group, while γ-irradiated PVA_a and PVA_b have lower Young's modulus (Figure 10 C, D). Furthermore, similar trend was observed between PVA_a and PVA_b groups whereby the

minimum bend radius value of EtO sterilized grafts were lower than the untreated PVA control group ($p \leq 0.05$ only for PVA_a group); while the γ-irradiated group minimum bend radii were in between untreated PVA control group and the EtO sterilized group with no statistical significance (Figure 10 E, F). In addition, burst pressure test of PVA_b group revealed a significant increase in burst pressure of the EtO sterilized PVA grafts ($p \leq 0.01$, n=4); while there were no significant differences found in either PVA_a group or γ-irradiated grafts of PVA_b group (Figure 10 G, H). Lastly, higher suture retention strength was observed also in EtO sterilized grafts of PVA_b group as compared to the untreated PVA grafts ($p \leq 0.01$, n=4). Similar trend was observed in PVA_a group but no statistical significance was found (Figure 10 I, J).

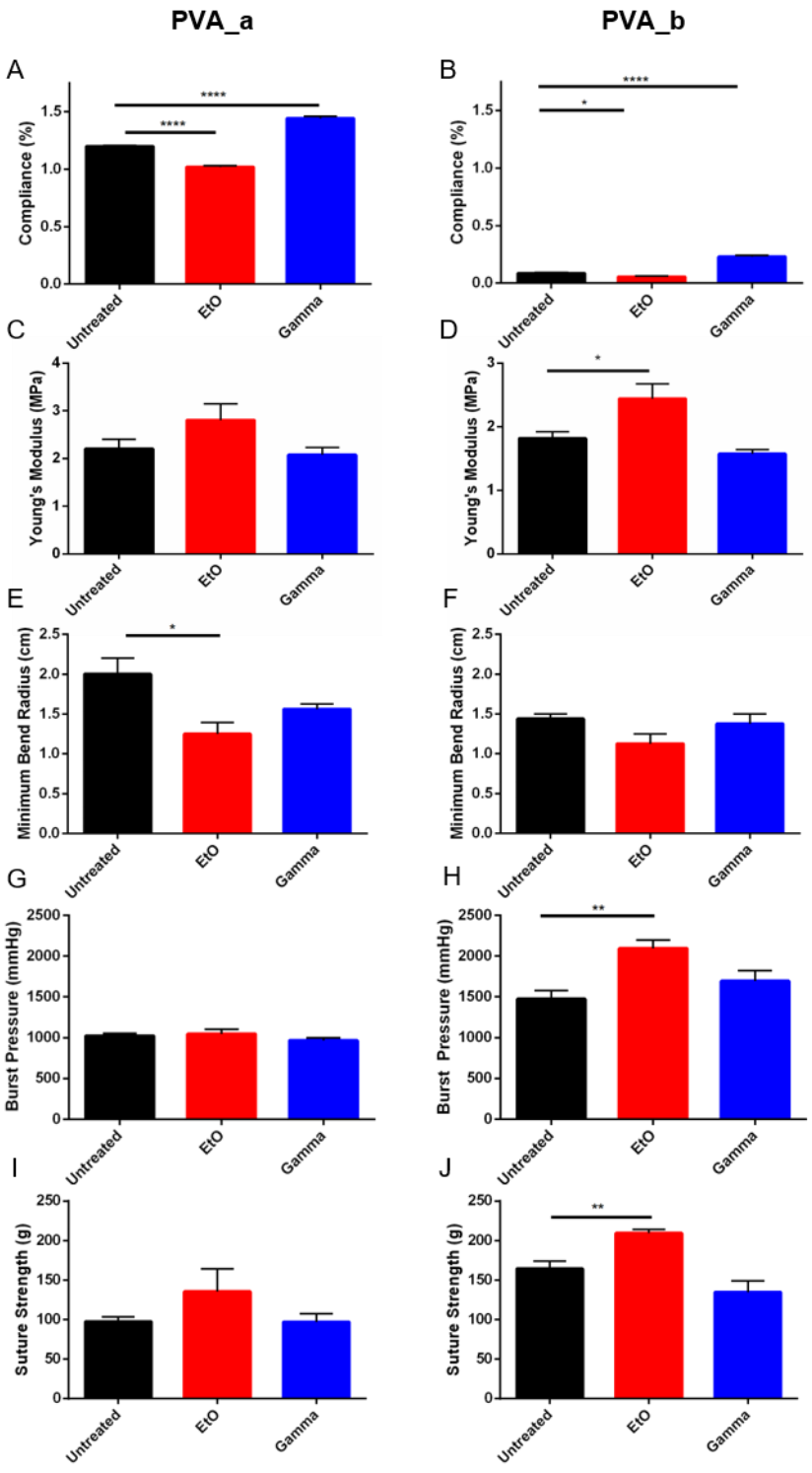

Figure 10. Changes in mechanical properties of PVA grafts after being sterilized with EtO and γ-radiation. Mechanical properties tested include: (A-B) compliance, (C-D) Young's modulus, (E-

F) minimum bend radius, (G-H) burst pressure, and (I-J) suture retention strength. Comparison of mean values with experimental replica, n=4.

3.3.3 Effect on PVA surface and chemical property

3.3.3.1 No observable difference on FTIR spectra of sterilized and non-sterilized PVA graft surfaces

FTIR was performed to assess any introduction of new ethoxyl function group on the graft surface due to ethoxylation reaction between EtO and –OH function group. From the measurement, we observed no new peak formed or loss after the sterilization process as shown in Figure 11. The peak intensity was found to be a result of measurement variation. Each sample group was measured in triplicate.

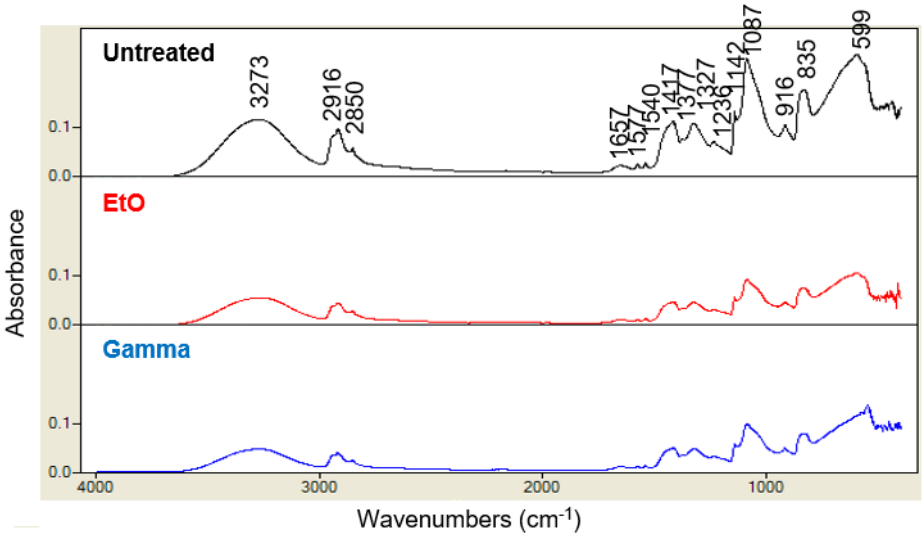

Figure 11. FTIR spectra of untreated, EtO, and γ-irradiated PVA grafts confirmed the absence/ insignificant presence of ethoxyl function group. No new peak formed or loss.

3.3.3.2 DSC curves of sterilized and non-sterilized PVA grafts show increase in PVA crystallinity

A significant increase in heat of fusion of the EtO sterilized grafts was observed ($p \leq 0.05$, n=3); while there was no significant change in the heat of fusion of γ-irradiated grafts (Figure 12). Heat of fusion is calculated from the area under exothermic peak of the second cooling cycle and is proportional to material crystallinity.

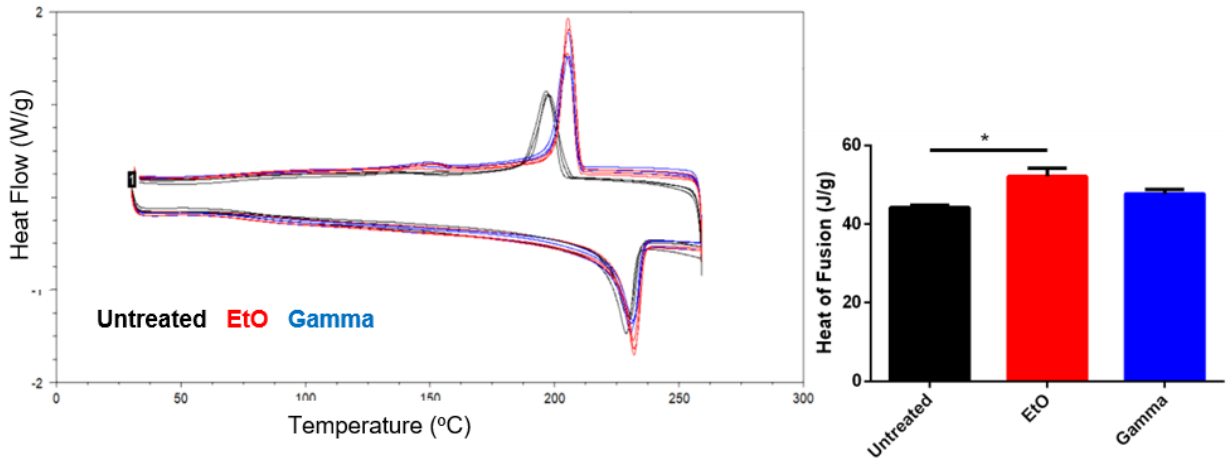

Figure 12. DSC result of untreated, EtO, and γ-irradiated PVA grafts. A significant increase in crystallinity was found in EtO sterilized grafts ($p \leq 0.05$, n=3).

3.3.3.3 Microgratings topography fidelity of sterilized and non-sterilized PVA surfaces was maintained

SEM imaging was performed to assess the fidelity of topography after EtO and γ-sterilization process. As shown in Figure 13, there was no observable change in surface roughness. More importantly, the fidelity of 2 μm gratings topography was maintained in both sterilization method.

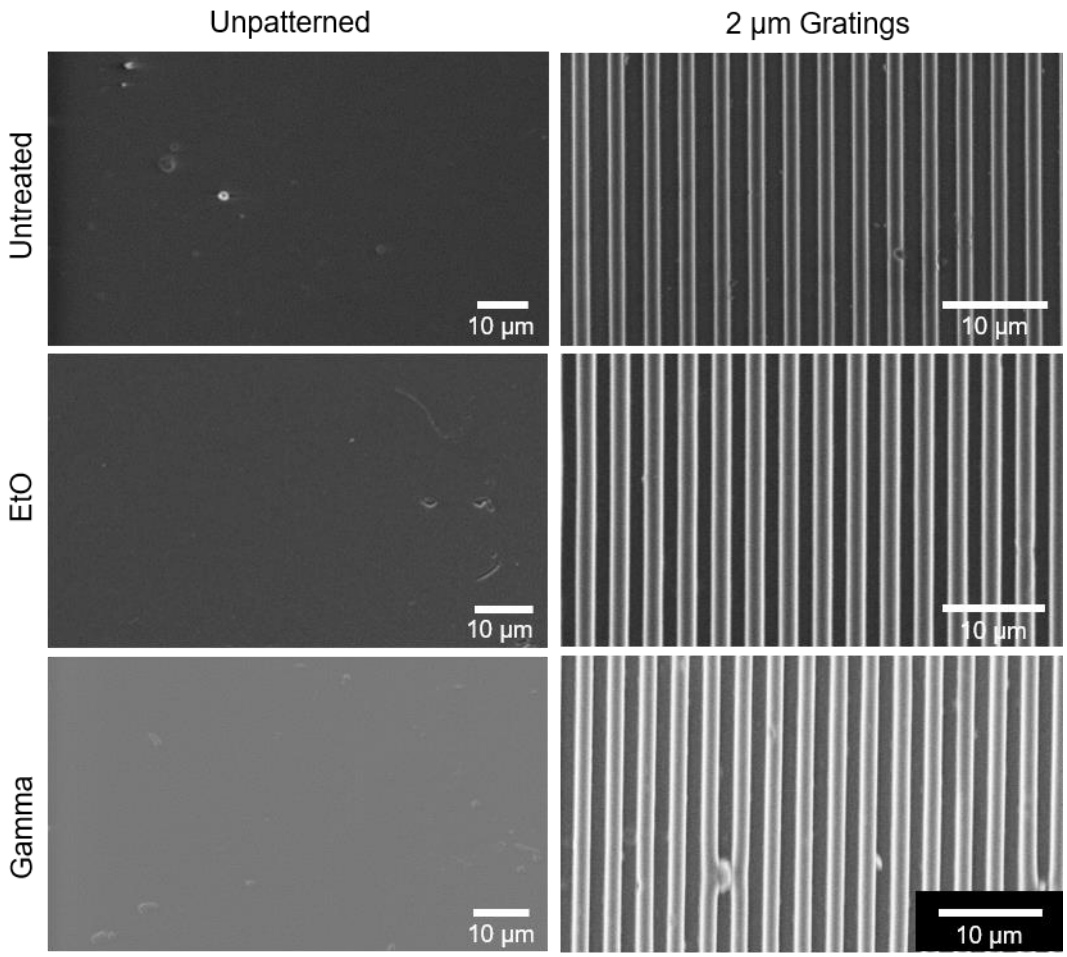

Figure 13. SEM images of unpatterned and PVA with 2 µm gratings topography after being sterilized with EtO and γ-radiation.

3.3.3.4 A decrease of oxygen percentage on γ-irradiated PVA film surface

A change in surface property of γ-irradiated PVA was observed from the XPS measurement result whereby the %O on the film surface was decreased compares to the untreated PVA group (Figure 14B). Similar trend was observed for the EtO sterilized PVA surfaces with a lesser extent. Due to this decrease, %C of both EtO and γ-irradiated PVA were slightly increased (Figure 14A); however, the increase was not statistically significant.

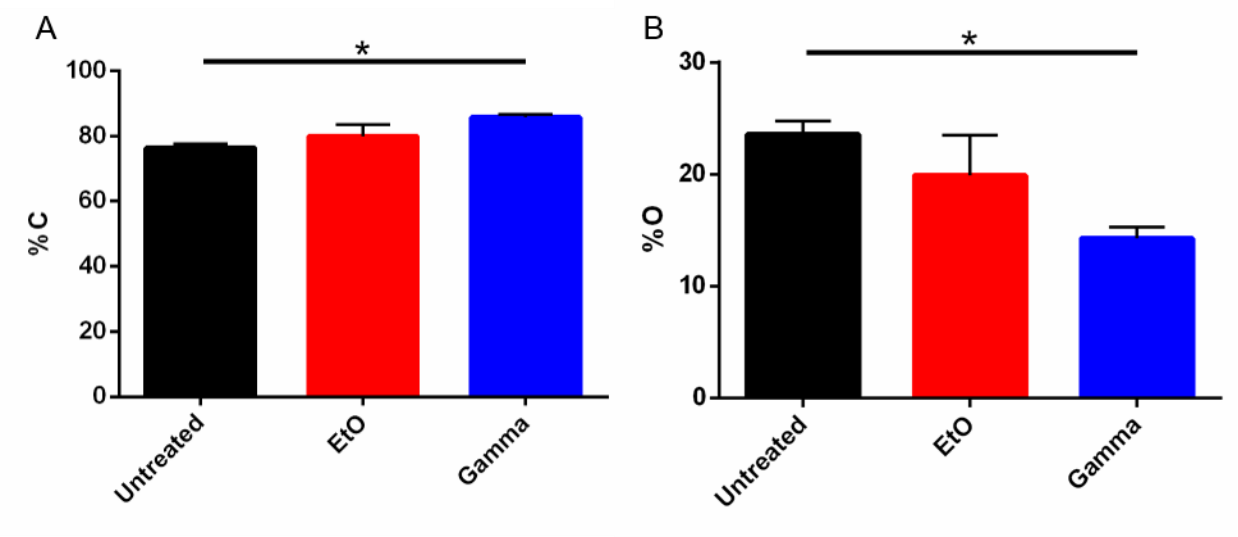

Figure 14. XPS measurement results showing (A) %C and (B) %O on the untreated and sterilized PVA surfaces. A significant increase and decrease in %C and %O respectively was observed on γ-irradiated PVA surfaces, n=3. * denotes statistical significance with p-value ≤ 0.05, comparison was performed against untreated PVA control.

3.3.3.4 Water contact angle measurement reveals significant change of γ-irradiated PVA film surface

The water contact angle of γ-irradiated PVA film was significantly increased compared to the untreated group (Figure 15) ($p \leq 0.05$, n=4). In contrast, the water contact angle of EtO sterilized PVA film was reduced but no statistical significance was found between the untreated group and EtO sterilized group. All tests were performed on unpatterned PVA films.

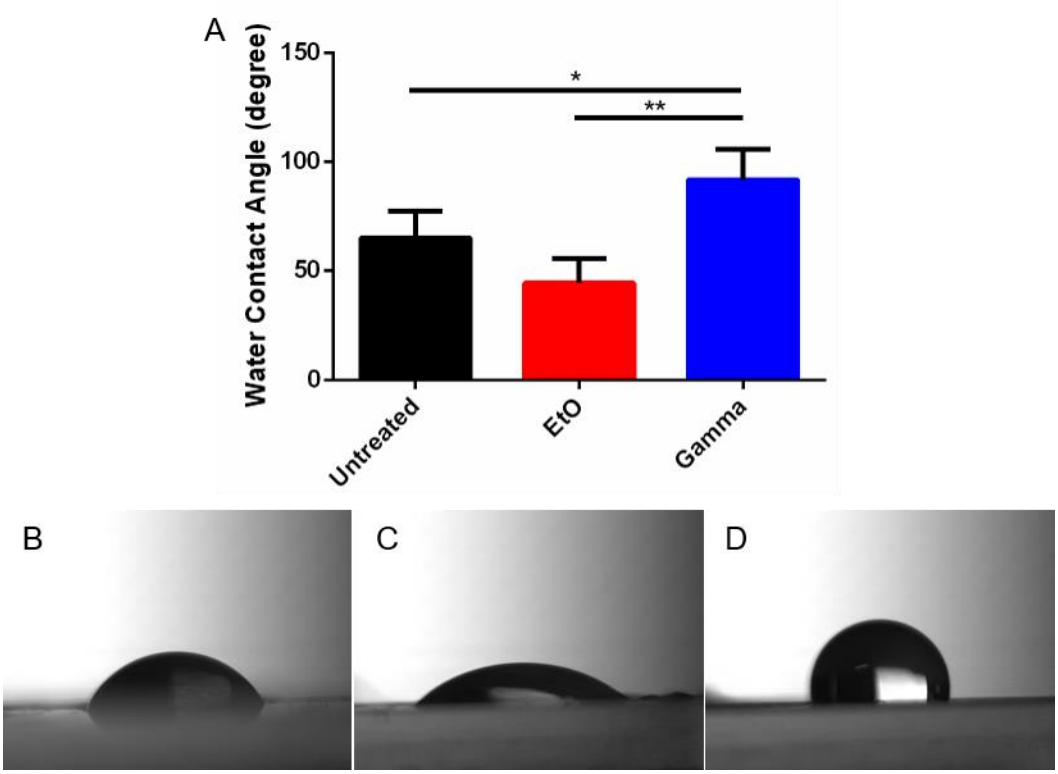

Figure 15. (A) Summary of PVA water contact angle and selected water contact angle images for (B) untreated PVA, (C) EtO sterilized PVA, and (D) γ-irradiated PVA groups. * represents statistical significance with p-value ≤ 0.05, ** p-value ≤ 0.01, n = 4.

3.3.4 Cellular study shows the non-toxic property of γ-irradiated PVA

The effect of PVA sterilization step, in particular γ-radiation, on endothelialisation was assessed by performing in vitro cell adhesion and toxicity study with EA.hy926. Cellular study was done with unpatterned PVA control and 2µm gratings PVA films, both with and without γ-radiation treatment. On day 14, endothelial monolayer was established on γ-irradiated PVA with 2µm gratings topography and the cells showed to have a clear alignment along the gratings parallel direction (Figure 16). Whereas on unpatterned PVA (with and without γ-radiation treatment) and 2µm gratings PVA without γ-radiation treatment, cells did not proliferate as fast and have a more rounded morphology. The cell number on 2µm gratings topography with γ-radiation treatment is

significantly higher than the other three groups, but still significantly lower than the cover slip controls ($p \leq 0.0001$, n=5) (Figure 14F). Hence, the γ-irradiated PVA surfaces were found to be nontoxic and to improve endothelialisation. No cell death was observed on the day of imaging.

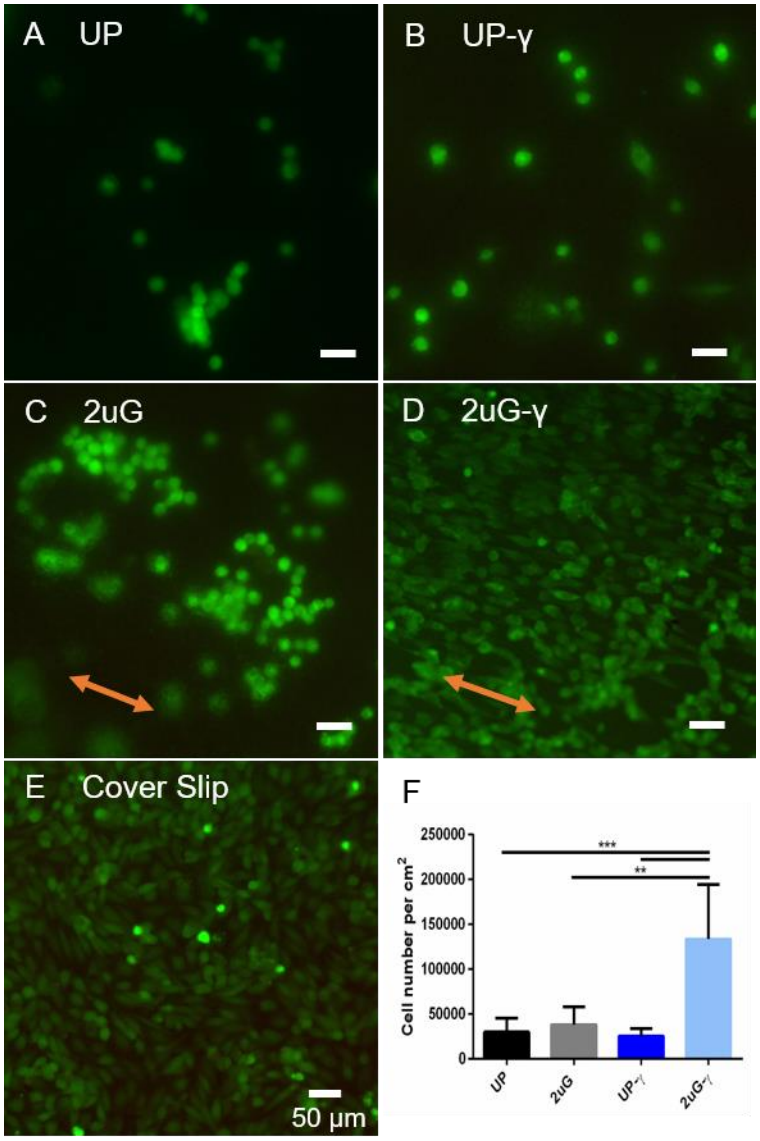

Figure 16. Live/dead staining of EA.hy926 cells on (A) unpatterned PVA without γ-radiation, (B) unpatterned PVA with γ-radiation, (C) 2 µm gratings PVA without γ-radiation, (D) 2 µm gratings PVA with γ-radiation, and (E) cover slip control after 13 days in culture. Orange arrows indicate the direction of gratings, scale bar: 50 µm. (F) Cell number quantification using CyQUANT® cell

proliferation assay kit showed a significant improvement in the number of adherent cells on 2 μm gratings PVA with γ-radiation (2uG-γ) compares to the other experimental groups (unpatterned PVA without γ-radiation (UP), 2 μm gratings PVA without γ-radiation (2uG), and unpatterned PVA with γ-radiation (UP-γ)). ** represents statistical significance with p-value ≤ 0.01, *** p-value ≤ 0.001, n=5.

3.4. Discussions

PVA grafts compliance was increased after γ-radiation treatment and decreased after EtO sterilization. This result is interesting and counter-intuitive as we would expect a more translucent graft to be more compliant. Moreover, weaker graft material would result in higher minimum bend radius (more easily kinked at higher degree of curvature); hence, the minimum bend radius result is in agreement with the compliance test result whereby the EtO sterilized grafts were found to be less compliant than the control group. In all the experimental groups, the measured burst pressure values were much higher than physiological blood pressure, which means that both sterilization method did not detrimentally affect the integrity of our PVA grafts and can be used for in vivo study. However, the mechanical property tests confirm that EtO sterilization affects PVA graft mechanical property more than γ-radiation and causes it to be stiffer after the treatment; whereas γ-radiation does not affect much on the mechanical property of PVA grafts except that it increased PVA graft compliance. Further characterization with FTIR was done to look into the presence of ethoxyl function group on the EtO sterilized PVA graft as well as to confirm any new peak formation or loss due to the sterilization process. Any significant addition of ethoxyl function would result in an increase of 2916 cm^{-1} peak which represents alkane function group. However, the FTIR spectra confirmed the absence/ insignificant presence of such function group which indicates that the EtO sterilized PVA grafts were safe to be used in vivo without any concern of

toxic residual. The interesting phenomenon with regards to the change in EtO sterilized graft opacity while at the same time having stiffer mechanical property is well-explained by the DSC spectra where an increase in the fractional crystallinity was observed. This change in crystallinity coming from EtO sterilization was interestingly observed by other group when sterilizing PLA fibers and was speculated to be caused by annealing effect during the sterilization process.[70]

As shown in the previous in vitro cell studies (chapter 2 and Cutiongco et al.[23]), 2 μm gratings topography provided the best cell attachment and some cells were even shown to align along the gratings direction which mimics the orientation of endothelial cells on the vessel lumen in vivo. Hence, understanding the effect of sterilization on the fidelity of 2 μm gratings topography is of our particular interest. As shown in Figure 12, the topography was still found to be well-oriented and this is likely contributed by lesser degree of freedom of the feature; while another study showed the disorientation of electrospun ribbons after EtO sterilization step.[70] Additionally, the aspect ratio of our 2 μm gratings topography is low (width: height = 1:1) and the disruption of surface topography may be more prominent in a higher aspect ratio.

PVA surface property was further characterized with XPS. Interestingly, a decrease in %O was observed especially on the γ-irradiated sample. This may indicate that some of the -OH function groups on the PVA surface was disrupted due to the radiation, and this finding is further supported by the water contact angle measurement of γ-irradiated PVA film (without pattern) which was significantly higher (more hydrophobic) compared to the untreated group (Figure 15). Since there was no observable change in surface roughness (Figure 13) and FTIR spectra (Figure 11), we suspect that the effect that γ-radiation has on the PVA graft is more superficial than the depth of penetration of the FTIR and involving chemical/ function group modification rather than physical.

From the characterization result above, we concluded that γ-radiation is a preferred sterilization method for PVA because it has minimal impact to PVA mechanical property and crystallinity. The in vitro cellular study was done on γ-irradiated and untreated PVA films, with and without 2 μm gratings topography. The significant increase in cell attachment on γ-irradiated surface with 2 μm gratings topography was consistently observed in all such samples (n=5). Given the water contact angle measurement of unpatterned γ-irradiated PVA surface and a previous water contact angle study done by our group on 2 μm gratings topography PVA surface, this could mean that the surface hydrophobicity of γ-irradiated 2 μm gratings surface was even higher and thus favors the adsorption of extracellular matrix protein which in turn facilitates cell attachment to ligands present in the extracellular matrix protein.

3.4 Conclusions

Sterilization methods such as EtO and γ-radiation are known to affect polymer mechanical integrity. Through this study, we have shown that mechanical compliance of STMP crosslinked PVA graft was significantly reduced by EtO sterilization and increased by γ-radiation. Other mechanical properties such as bend radius, burst pressure, suture retention strength were not greatly affected but showed consistent trend with the mechanical compliance data. Additionally, crystallization of EtO treated PVA was shown to be significantly increased. Although the FTIR spectra did not show any peak formation and loss, the XPS and water contact angle measurement revealed the change in surface property of the sterilized PVA surfaces. It is interesting to see that rather having poor cell proliferation on the γ-irradiated PVA due to toxicity, 2 μm gratings topography with γ-radiation treatment show a significant cell adhesion and proliferation improvement. To conclude, γ-radiation is a more preferred sterilization method for STMP

crosslinked PVA graft due to its minute effect on PVA graft mechanical properties and the significant improvement in surface endothelialisation.

CHAPTER 4

In vivo Study of PVA Vascular Grafts

4.1 Introduction

Our group has previously implanted small diameter PVA vascular grafts in rabbit femoral artery with the 15-day patency rate of 67%.[22] Gamma irradiated grafts with 4 mm length and 0.9 to 1 mm ID were implanted with end-to-end anastomosis configuration. More importantly in at least one of the patent grafts, graft luminal surface endothelialisation was observed. Although this result is encouraging, there are still several challenges to nail down. Firstly, an end-to-side anastomosis configuration will be a more relevant model for a small diameter bypass vascular graft compares to an end-to-end anastomosis configuration. However, implantation of a 2 mm inner diameter synthetic vascular graft in end-to-side anastomosis configuration has rarely, if not never, been done before. A few studies performing end-to-side anastomosis between two adjacent vessels or using a decellularized allograft were reported previously.[78-81] However, implantation of synthetic vascular graft posts a more challenging problem in that graft and artery thickness do not always match which makes it difficult to suture the two in an end-to-side configuration. Secondly, endothelialisation of longer graft length would take longer which gives rise to a question of whether the graft will remain patent throughout the duration of implant when graft endothelialisation does not occur fast enough and thrombogenesis could take place. Thirdly, longer implant duration would give an opportunity for the formation of intimal hyperplasia and thrombus which again gives rise to the issue of graft patency rate.

One persistent issue with a small diameter vascular graft is the formation of neointima/intimal hyperplasia (IH) at graft anastomoses which causes stenosis and subsequent graft failure. There are at least two causes of IH which are widely believed by the cardiovascular society. The first cause is the wall shear stress (oscillatory, shear stress gradient) which in most cases is unavoidable; for example, the inflexion in bypass vascular graft configuration which cause

the blood flow profile to be skewed to the internal side of the graft closer to the native vessel. The second cause is vessel injury which results from a mismatch in mechanical compliance between graft material and native vessel, creating a high stress region at the suture line when graft and vessel is under pulsation. Later studies have also reported the importance of suturing technique to the compliance at the anastomosis region which can affect the hemodynamic of blood in and out of the vascular graft. Generally, both interrupted and continuous suturing will create a para anastomotic hypercompliant zone (PHZ) within 1-4 mm width from the suture line with the latter having a greater magnitude of PHZ.[82]

To answer the question of whether small diameter PVA vascular graft can stay patent given the listed challenges above and to achieve a success in future clinical trial, in vivo studies using animal model are necessary.

The tendency of neointima formation varies between species. Rabbit was chosen among other small animal models because its hemodynamic and hemostatic mechanism resembles human's the most.[83] In addition, bigger diameter vessel would represent a better model for intimal hyperplasia study due to the blood flow and shear stress experienced by the vessel. Hence, rabbit carotid artery was chosen as the implant site. The mechanical property of rabbit carotid artery in comparison to human brachial artery and PVA graft is shown in Table 4. Human brachial artery is chosen as an example of small diameter vessel in the extremities.

Table 5. Comparison of mechanical properties between PVA graft, rabbit carotid artery and human brachial artery

Properties	**PVA graft**	**Rabbit carotid artery**	**Human brachial artery**
Internal diameter (mm)	≤1 to 6	1.9 to 2.1 [83]	3.44 to 4.42 [84]
Compliance (%/40 mmHg)	1.5 to 9	3.1 [85]	1.3 to 3.3 [86]

Young's modulus (Pa)	2-8 x 10^5	6.45 x 10^{6} [87]	1.0 x 10^{5} [88]
Suture retention (g)	83 to 200	Not available	Not available

Having all the challenges and literature studies in mind, we hypothesize that a longer small diameter PVA graft can be implanted in end-to-side anastomosis configuration and maintain its patency throughout 28- to 30-day implant duration in rabbit carotid artery. Furthermore, we hypothesize that there will be no observable inflammation reaction at the end of implant duration.

4.2 Materials and Methods

4.2.1 Animal handling and animal care committee approval

Vascular graft implants in male New Zealand White rabbits (*Oryctolagus cuniculus*, 3.7±0.2kg) were performed at the Center of Animal Facility (CAF) at the University of Waterloo. Studies were approved (#AUPP 16-09) by the Animal Care Committee according to the Canadian Council on Animal Care's Guidelines, the requirements of Province of Ontario's Animals for Research Act, and the University of Waterloo's Guidelines for the Use of Animals in Research and Teaching. CAF was accredited by the Ontario Ministry of Agriculture and Food and Rural Affairs with accreditation number 0079-01 and was certified by the Canadian Council on Animal Care to have a Good Animal Practice. Baytril (enrofloxacin), 10 mg/kg (Bayer) was administered intramuscularly as antibiotic 24hrs before surgery. The rabbit was introduced to isoflurane. Narketan (ketamine), 35mg/kg (Vetoquinol) and Xylazine (5mg/kg) administered intramuscularly was used for anaesthesia. Heparin, 200 IU/kg (Sandoz) was given intravenously prior to arterial clamping. In the event of vasoconstriction or spasm of the arteries, 5-10mL of warm (37°C), sterile saline solution was applied topically on the constricted vessel. If vasodilation was not observed, a few drops (0.3-0.5mL) of Papaverine (a vasodilator) were applied topically on the vessel.

4.2.2 Anastomosis technique

Both PVA (ID: 1.8 mm, length: 1.9 cm) and ePTFE (ID: 2 mm, length: 1.9 cm) grafts were both pre-cut in oblique manner (45^{o}) to the graft long axis. Rabbit right common carotid artery (CCA) was exposed and papaverine (DBL) was applied topically to prevent spasm. Any side branches found on the common carotid artery was then ligated. Two vascular clamps of size 3 were used to clamp the common carotid artery at cranial and caudal positions. To make an end-to-side anastomosis, a hole was made at the CCA by creating a knot at the vessel wall and then cutting away the knotted section. Using 8-0 Ethilon Polyamide 6 suture (Ethicon), the graft was stitched onto the vessel with 8-10 interrupted suture knots starting with 1 knot on each cranial (position 1 in Figure 15B) and caudal side (position 2, 180^{o} apart from position 1) and followed by 3-4 knots on each of the lateral and ventral side. After finishing the second end-to-side anastomosis, the mid-section of the CCA was tied with 2 knots to encourage blood flow through the graft and clamps were then released for leak test.

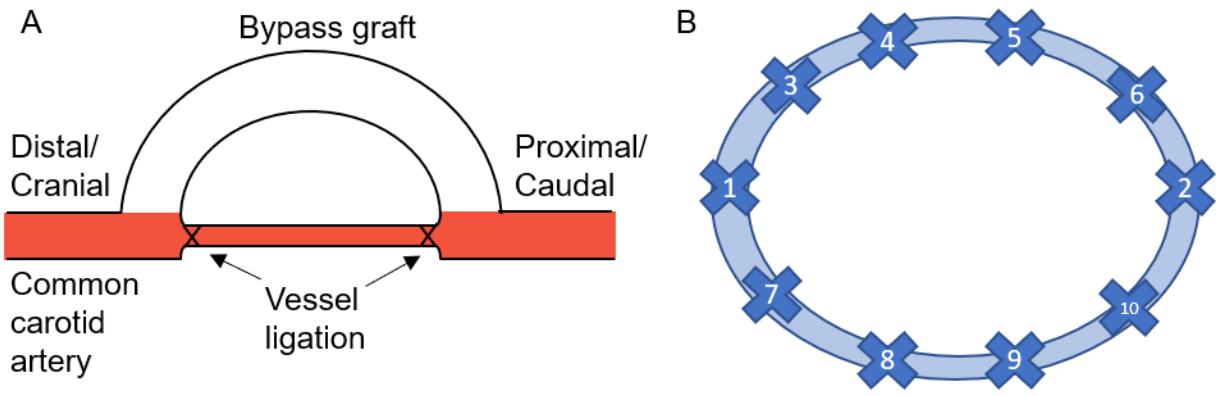

Figure 17. Schematic of (A) bypass graft implant at the common carotid artery with end-to-side anastomosis technique and (B) graft cross-section facing the common carotid artery with the order and positions of interrupted sutures indicated around the graft.

4.2.3 Ultrasound doppler

To assess patency of the implanted grafts, ultrasound doppler imaging and measurements were done on day 10-17 (midpoint) and on day 28-30 (endpoint). Measurements were performed using SonixTouch (Analogic Ultrasound, Peabody) and 10.0 MHz probe. Rabbit was put under 1-2% isofluorane prior to performing ultrasound measurement.

4.2.4 Histology of the excised grafts

Heparin (500 IU) was administered into the blood circulation prior to euthanization with sodium pentobarbital (100 mg/kg). The graft, CCA, and surrounding tissues were excised and fixed in 4% paraformaldehyde for 72 hours. Tissue was then sectioned according to the dashed lines shown in Figure 18. Moreover, tissue embedding was done using Paraplast (Leica) with the determined cutting plane facing upwards (see Figure). Tissue slides were stained with standard hematoxylin and eosin (H&E) for imaging. To visualize the tissue, 4x and 10x magnification were used to get an overall and close up view respectively.

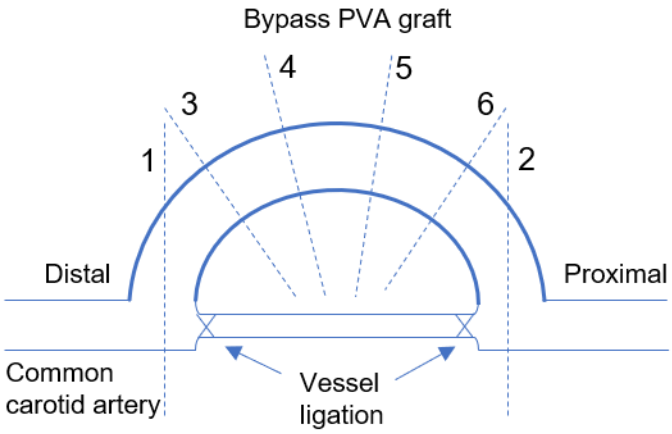

Figure 18. Tissue sectioning map for histology samples.

4.3 Results and Discussions

PVA grafts used in this in vivo study have similar dimension to PVA_a in chapter 3. However, to cater for the bypass grafting configuration, PVA grafts were curved at the middle section. The compliance value of the low compliance (LC) PVA group was 1.29 ± 0.27%/ 40mmHg, while the compliance value of the high compliance (HC) PVA group was 1.95 ± 0.62%/ 40mmHg. The ePTFE grafts (2mm) used in this study have a slightly bigger diameter than the PVA grafts (1.8mm). The compliance of these ePTFE grafts was 3.08 ± 1.49%/ 40mmHg. The end-to-side anastomosis configuration was successfully done (Figure 19) with interrupted suture technique using 8-0 Ethilon Polyamide 6 suture with the suturing order as illustrated in Figure 17. The advantage of suturing position 1 and 2 first is to avoid misalignment of graft which potentially could cause kinking on the graft. Although the duration in completing one anastomosis is relatively longer for an interrupted suturing technique than a continuous suturing technique, interrupted is still preferred since continuous suturing technique can produce a purse-string effect and impair haemodynamic effect at the anastomosis; it can also exaggerate PHZ.[82] Also, another advantage of doing interrupted suture is allowing to redo any suture at one position without disrupting other sutures. At the endpoint, sutures were found to stay in their original positions.

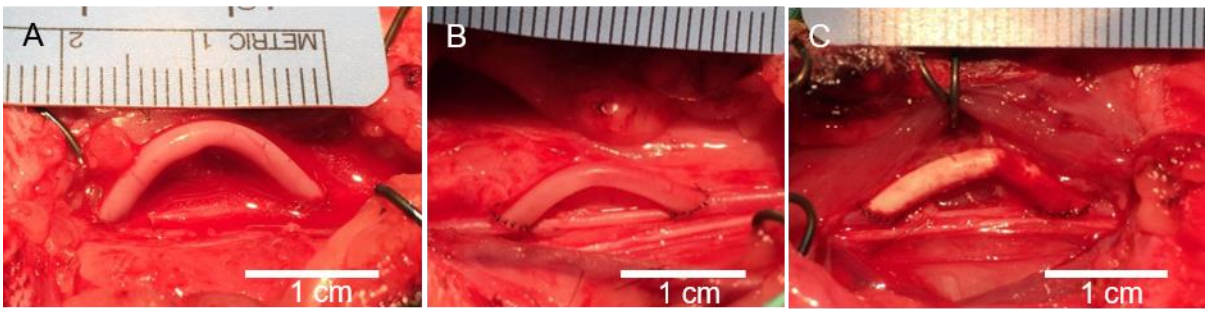

Figure 19. Day 0 images of PVA grafts (A-B) and ePTFE graft (C) right after surgery. PVA graft in (A) has lower compliance and thicker graft wall than in (B).

In the study period, 10 rabbits underwent 10 carotid bypass surgeries. All rabbits survived until the endpoint (28-30 days). One out of 10 rabbits had an edema after the procedure but eventually recovered after getting hot and cold compression for 2 consecutive days. Another rabbit was identified to have a slow right eye response and flopped ear after the surgery, but the overall being was healthy regardless. Out of the 10 grafts that were implanted, only 9 grafts were analyzed because one graft was found in kinked condition at the time of tissue excision and there was no blood flowing through it. The 9 grafts that were analyzed consist of 3 low compliance (LC) PVA grafts, 4 high compliance (HC) PVA grafts, and 2 ePTFE graft. Two out of 3 LC PVA grafts and 3 out of 4 HC PVA grafts were partially patent, while 1 out of 2 ePTFE grafts was patent. PVA grafts with lower compliance yielded a lower 28- to 30-day patency rate (67%) than PVA grafts with higher compliance (75%).

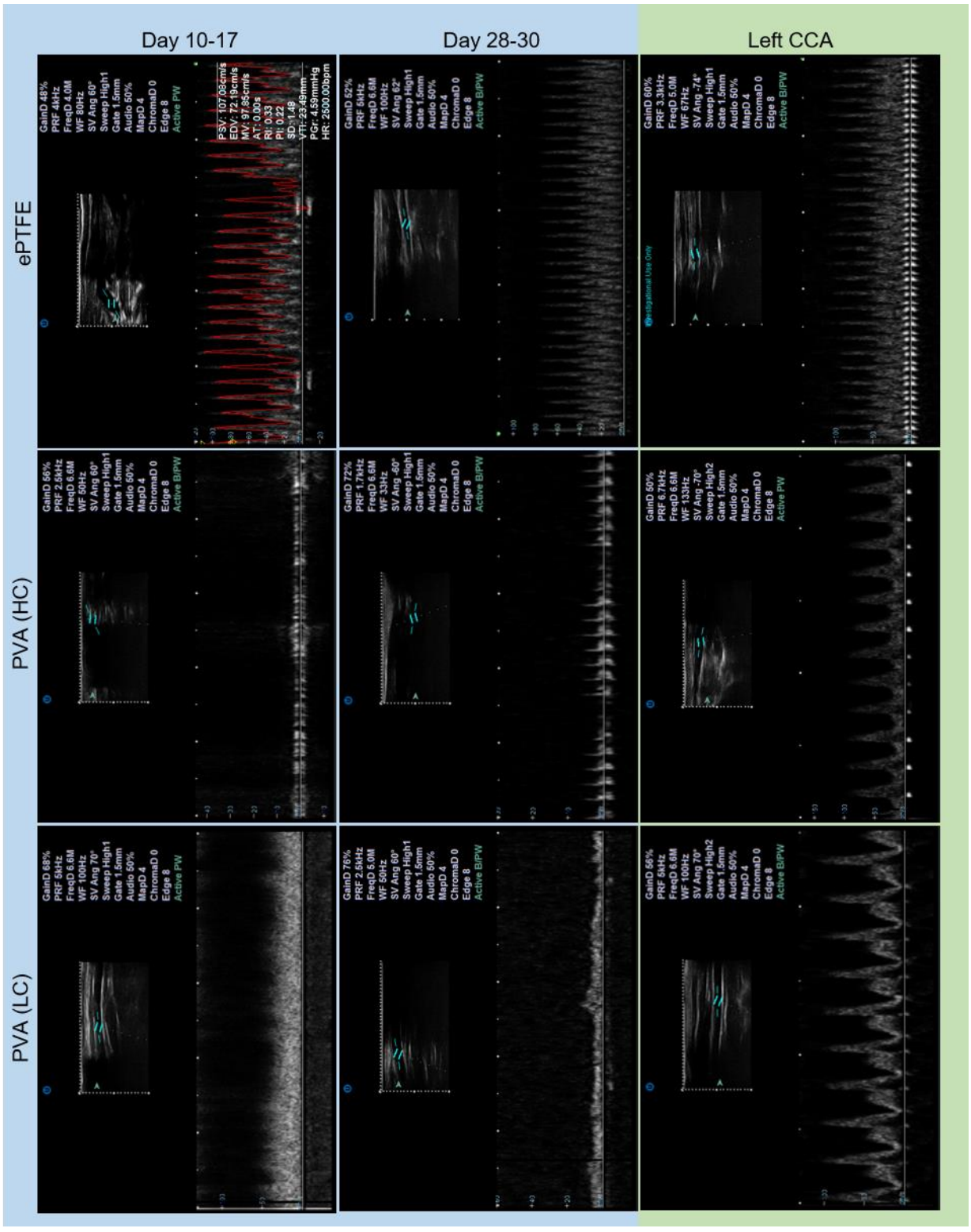

Figure 20. Ultrasound flow measurement (M-mode) of the PVA grafts (HC and LC) and ePTFE graft at midpoint (day 10-17), endpoint (day 28-30), and their corresponding controls, unoperated

left common carotid artery (left CCA). Control flow velocity did not change much from midpoint measurement to endpoint measurement.

Ultrasound flow measurement was performed on all the 8 grafts that were implanted at the midpoint (day 10 to 17 after surgery) and the endpoint (day 28-30 after surgery) (Figure 19). It is important to note that rabbit to rabbit blood flow rate variation, as assessed from the unoperated side of the common carotid artery, can be quite substantial even with the similar dose of anaesthetics. Hence, for the analysis, we are reporting relative volumetric flow rate, that is, the ratio between volumetric flow rate of PVA graft and of the unoperated contralateral control. Seven out of 7 PVA grafts and 1 out of 2 ePTFE grafts are still patent at the midpoint ultrasound measurement. In 5 out of 7 PVA grafts, a decrease in relative volumetric flow rate from the midpoint measurement to the endpoint measurement was observed (see Table 5). The increase in volumetric flow rate ratio of rabbit #5 and #6 could be caused by measurement errors. IH or thrombus formation could be the main issue causing graft stenosis and flow decrease over time. Also, it was apparent in one of the grafts that the stenosis was worse at the distal anastomosis rather than proximal as the flow profile showed an increase in flow velocity from proximal to distal end (Figure 21). Percent stenosis values in Table 6 were calculated from the cross-section area of tissue ingrowth covering the graft lumen; where a 100% stenosis indicates complete obstruction to the blood flow by the tissue ingrowth. In the case of rabbit #3, graft was occluded at the endpoint due to both tissue ingrowth and thrombus. All values in Table 6 have 3 significant figures.

Table 6. Summary of graft compliance, normalized volumetric flowrate, and corresponding percent stenosis

Graft Type	Rabbit #	Volumetric Flowrate of Graft on Day 10-17 (ml/sec)	Relative Volumetric Flowrate on Day 10-17	Volumetric Flowrate of Graft on Day 28-30 (ml/sec)	Relative Volumetric Flowrate on Day 28-30	% Stenosis (Distal)	% Stenosis (Proximal)
PVA (LC)	1	1.29	4.61×10^{-1}	3.91×10^{-1}	1.40×10^{-1}	18.8	0
	3	2.77×10^{-1}	8.10×10^{-2}	Occluded	Occluded	87.8 (occluded)	86.3 (occluded)
	5	1.25×10^{-2}	4.41×10^{-3}	8.58×10^{-3}	5.16×10^{-3}	20.1	8.48
PVA (HC)	2	3.98×10^{-2}	2.30×10^{-2}	5.50×10^{-3}	3.18×10^{-3}	100 (occluded)	Data not available[a]
	4	1.55	3.34×10^{-1}	1.86×10^{-3}	2.98×10^{-4}	0.282	0
	6	1.53×10^{-2}	4.33×10^{-3}	3.22×10^{-1}	6.58×10^{-2}	0.378	28.4
	8	1.74×10^{-1}	1.10×10^{-1}	2.72×10^{-2}	1.34×10^{-2}	2.65	7.09
ePTFE	7	4.73	2.68	1.29	6.45×10^{-1}	31.6	38.9
	9	Occluded	Occluded	Data not available[b]	Data not available[b]	96.3 (occluded)	92.6 (occluded)

(a) Measurement is unable to be done due to unsuccessful tissue sectioning.
(b) Ultrasound measurement was not done.

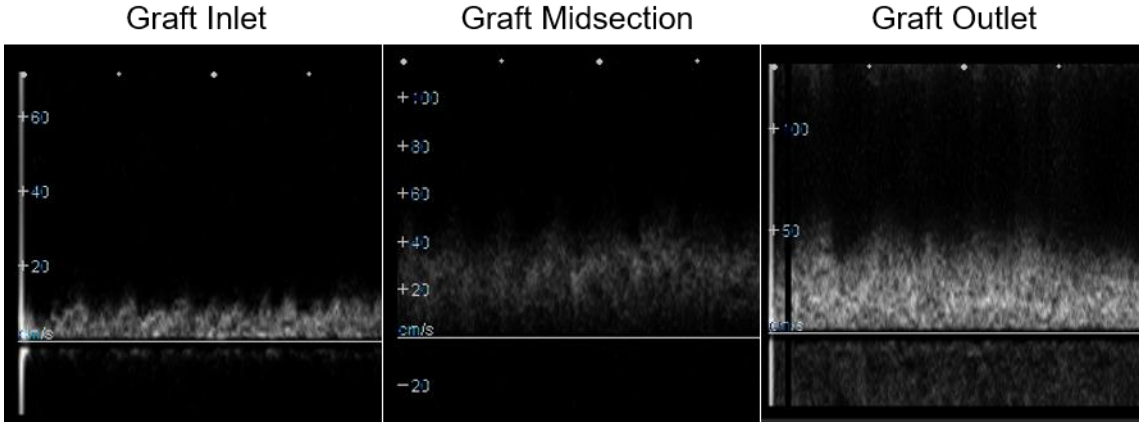

Figure 21. Ultrasound measurement of flow velocity versus time shows an increase in magnitude from graft inlet to graft outlet.

Figure 22 shows the hematoxylin and eosin (H&E) staining of excised vascular graft at point 1 or 2 according to tissue sectioning map shown in Figure 18. Based on the H&E staining of the tissue sections, there was no observable inflammatory reaction found from any of the excised tissues. Interestingly, the anastomoses sections (both distal and proximal) showed that IH was formed mainly on the native artery close to the heel and bed regions and not on the PVA graft lumen (Figure 22 A, B). The heel and bed regions are expected to be close to one another due to the position of vessel ligation (indicated with small x in Figure 17 and 18). Unlike tissue response towards PVA grafts, neointima tissue was observed to grow and attach well on the ePTFE grafts (Figure 22 E, F, G, H). Furthermore, tissue encapsulation was found around the excised ePTFE grafts and was inseparable from the grafts. We suspect that due to animal to animal variation, the tissue response on the two implanted ePTFE grafts was different and resulted in one graft being patent (Figure 22 E, F), while the other being occluded (Figure 22 G, H). Moreover, in some of the PVA samples, thrombus was found attaching on the IH tissue of the native artery, while in some others it was observed to be present on the graft lumen (Figure 22 C, D). This thrombus can either form during the animal lifetime or post-mortem since tissue excision and fixation happened after the animals were euthanized. However, the first could also be one reason for the absence of correlation between blood flow rate ratio and graft compliance, while blood flow rate ratio should be a good indication of stenosis level at the anastomoses of the grafts. This is also supported by the fact that endothelialisation was not found in any of the PVA graft lumen.

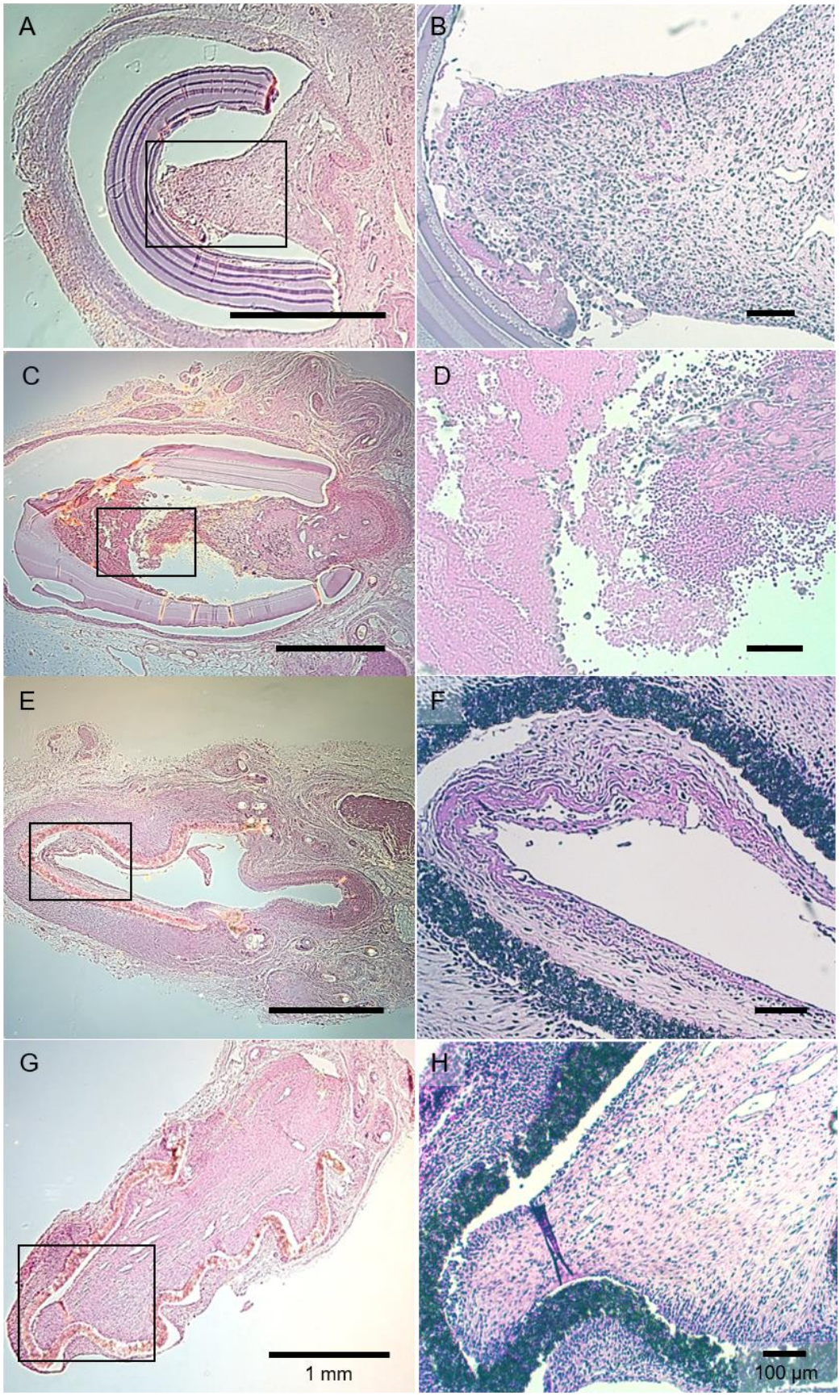
A
B
C
D
E
F
G
H
1 mm
100 µm

Figure 22. H&E staining of anastomoses tissue sections with their respective magnified images of the bounded area shown on the right. (A) Patent PVA graft, (B) corresponding magnified view shows the presence of intima tissues growing from the native artery, (C) PVA graft with thrombus, (D) corresponding magnified view of the thrombus, (E) patent ePTFE graft, (F) corresponding magnified view shows the presence of intima tissues on the graft lumen, (G) occluded ePTFE graft, (H) corresponding magnified view shows the growth of intima tissues covering graft lumen. Scale bar of Figure 21 A, C, E, G is 1 mm, while scale bar of Figure 21 B, D, F, H is 100 μm.

As for the correlation between PVA graft compliance and IH formation, our preliminary observation found that the percent stenosis increased as the graft compliance value increased which seems to be contrary to the common belief (see Figure 23). Graft compliance value in this study ranges from 1.1±0.5%/40mmHg to 2.8±0.4%/40mmHg, while carotid artery compliance was measured with the same in vitro compliance test method and the compliance value was 2.57±0.04%/40mmHg (n=1), which is close to the compliance value found by another group.[88] One outlier (rabbit #4) was found and was identified to be caused by the angle of implant which was much less than 45^{o} angle and caused a more favorable hemodynamic (less wall shear stress) at the region around the anastomoses.

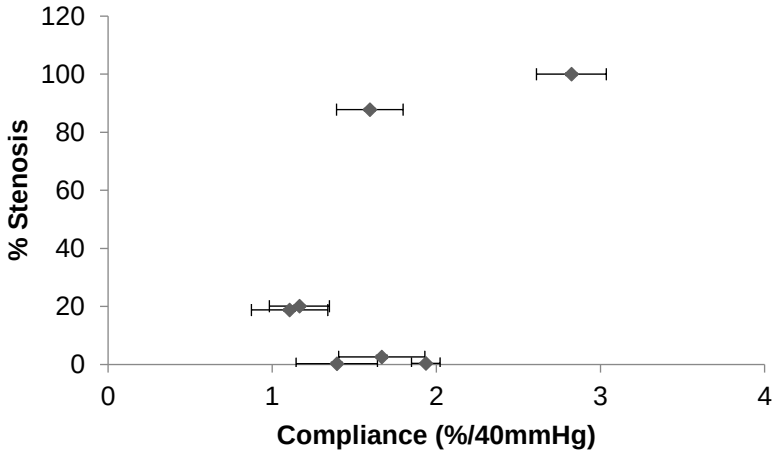

Figure 23. Scatter plot of PVA graft compliance against percent stenosis at distal anastomoses. Each point represents one sample and the error bars (SD) were calculated from up to 7 measurement points along each of the PVA graft sample.

This preliminary finding prompted us to look into physiological stress factor that could affect the artery compliance and the stress-strain profile our PVA grafts. In physiological condition, an artery is always under pre-tension; a study on rabbit femoral arteries revealed that the pre-tension force that was experienced is 0.113 ± 0.038 N when limb was extended, 0.071 ± 0.014 N when limb was relaxed.[89] Also according to the data found by Fung, et al., the pre-tension force places an artery to be at 50% axial stretching, which contributes to the difference in vessel compliance in vivo.[90] The viscoelasticity of an artery makes it stronger radially as higher force is applied longitudinally. In this study, we implanted PVA grafts in end-to-side anastomoses configuration; as the grafts are in curved position when implanted, they have more degrees of freedom and less pre-tension force. The measurement of graft pre-tension force in vivo is outside the scope of this thesis; however, based on the ultrasound flow measurement and histology results, we predict that PVA grafts with lower compliance value match better the compliance of rabbit common carotid artery in vivo, resulted in higher patency rate; whereas grafts with higher (matching) compliance value have higher distensibility than the artery and invoke neointima response more severely. Furthermore, Ballyk et al. shows that end-to-side anastomosis of a vein graft (higher compliance) applied more stress on the suture line compared to artery graft (lower compliance); although Dacron graft applied even higher stress on the suture line than both artery and vein graft.[6] This could mean that the force experienced by the vessel depends heavily on the graft material property and not just a simple compliance to IH relation. Nevertheless, our preliminary observation on the IH formation is based on a rather small sample size and statistical

analysis could not be performed. Given a large variation between the animals, a larger sample size is required to confirm this finding.

4.4 Conclusions

In conclusion, we have successfully implanted small diameter PVA grafts in an end-to-side anastomosis configuration. We found that the overall 28- to 30- day patency of PVA grafts (1.9 cm long, 2 mm ID) was as high as 71% and there was no inflammatory reaction found. However, endothelialisation on the graft lumen was not observed which could be the reason of thrombus formation in graft lumen. The correlation of IH formation and graft compliance is at the moment inconclusive due to the sample size. Further study is required to confirm this finding.

CHAPTER 5

General Conclusions and Recommendations

5.1 General conclusions

Endothelialisation of a vascular graft can help to improve graft patency by preventing platelet and coagulation factors activation. As the performance of small diameter ePTFE graft has been disappointing, many other synthetic and composite materials were explored among which STMP-crosslinked PVA was chosen to be a promising material to make a small diameter vascular graft. However, surface property of PVA needs to be altered to allow for endothelialisation in vitro and in vivo. This alteration was done through luminal plasma modification with NH_3 plasma coupled with surface microtopography 2x2x2 μm gratings and 1.8 μm concave lenses, as both topographies were shown previously to have a positive effect on endothelial cell adhesion.[23] This thesis has shown the potential of NH_3 luminal plasma treatment in further improving cell adherence without compromising hemocompatibility of PVA grafts. The sterilization study with EtO and γ-radiation was conducted to determine the best sterilization method for sterilizing our PVA grafts. As shown in sterilization of other materials, EtO sterilization changes PVA crystallinity and mechanical property, while γ-radiation does not. More importantly, γ-radiation increases water contact angle of PVA and endothelial cell attachment on γ-irradiated 2 μm gratings PVA surface was significantly higher than the untreated substrates (with and without pattern) and γ-irradiated unpatterned PVA. With the decent improvement in the in vitro endothelialisation of PVA and the identification of a suitable sterilization method, small diameter PVA vascular grafts were implanted at the rabbit common carotid arteries with an end-to-side anastomosis configuration. PVA grafts that were used in this study were unpatterned, γ-irradiated PVA grafts with two different compliance ranges for gathering preliminary data on the IH formation. The main aim of the in vivo study is to assess whether the longer small diameter PVA graft without surface topography could maintain its patency after 28 to 30 days and be endothelialised in vivo without

any inflammatory response as cell response to biomaterial surface in vivo may vary from in vitro. The 28- to 30-day patency rate of the unpatterned PVA was as high as 71% and no inflammatory response was observed. However, endothelialisation on graft lumen was not observed.

5.2 Recommendations

Future direction for this thesis work will be to incorporate luminal modification, i.e. NH_3 plasma treatment and/ or 2 μm gratings topography into the small diameter PVA grafts for the in vivo study. The in vivo study is still ongoing and eventually sufficient number of animals per experimental group will be achieved and statistical significance of the results will be obtained. Further improvement on graft patency could be done through identifying the ideal compliance range that could minimize IH formation. Vessel ligation should also be made further from the anastomosis region to avoid exaggeration of IH formation on the native artery and to allow a better assessment of the IH formation on the PVA graft lumen. It is also important to have the means to accurately measure the in vivo compliance of the carotid vessel to further evaluate the graft-vessel compliance mismatch in vivo.

References

1. Kirkwood, M. L.; Wang, G. J.; Jackson, B. M.; Golden, M. A.; Fairman, R. M.; Woo, E. Y., Lower limb revascularization for PAD using a heparin-coated PTFE conduit. *Vascular and endovascular surgery* **2011,** *45* (4), 329-34.
2. Organization, W. H. The top 10 causes of death. http://www.who.int/mediacentre/factsheets/fs310/en/ (accessed 17 March).
3. Hemmasizadeh, A.; Darvish, K.; Autieri, M., Characterization of changes to the mechanical properties of arteries due to cold storage using nanoindentation tests. *Annals of Biomedical Engineering* **2012,** *40* (7), 1434-42.
4. Gong, W.; Lei, D.; Li, S.; Huang, P.; Qi, Q.; Sun, Y.; Zhang, Y.; Wang, Z.; You, Z.; Ye, X.; Zhao, Q., Hybrid small-diameter vascular grafts: anti-expansion effect of electrospun poly e-caprolactone on heparin-coated decellularized matrices. *Biomaterials* **2016,** *76*, 359-70.
5. Salacinski, H. J.; Goldner S Fau - Giudiceandrea, A.; Giudiceandrea A Fau - Hamilton, G.; Hamilton G Fau - Seifalian, A. M.; Seifalian Am Fau - Edwards, A.; Edwards A Fau - Carson, R. J.; Carson, R. J., The mechanical behavior of vascular grafts: a review. (0885-3282 (Print)).
6. Ballyk, P. D.; Walsh, C.; Butany, J.; Ojha, M., Compliance mismatch may promote graft-artery intimal hyperplasia by altering suture-line stresses. *Journal of biomechanics* **1998,** *31* (3), 229-37.
7. Walden, R.; L'Italien, G. J.; Megerman, J.; Abbott, W. M., Matched elastic properties and successful arterial grafting. *Archives of surgery* **1980,** *115* (10), 1166-9.
8. Jerjes-Sanchez, C., Venous and arterial thrombosis: a continuous spectrum of the same disease? *European Heart Journal* **2005,** *26* (1), 3-4.
9. Lip Gy Fau - Blann, A. D.; Blann, A. D., Thrombogenesis and fibrinolysis in acute coronary syndromes. Important facets of a prothrombotic or hypercoagulable state? (0735-1097 (Print)).
10. Feletou, M., Part 1: Multiple Functions of the Endothelial Cells—Focus on Endothelium-Derived Vasoactive Mediators. In *The Endothelium*, Morgan & Claypool Life Sciences: San Rafael (CA), 2011.
11. Michiels, C., Endothelial cell functions. *Journal of cellular physiology* **2003,** *196* (3), 430-443.
12. Allaire, M. D. E.; Clowes, M. D. A. W., Endothelial Cell Injury in Cardiovascular Surgery: The Intimal Hyperplastic Response. *The Annals of thoracic surgery* **1997,** *63* (2), 582-591.
13. Tordoir, J. H.; Hofstra L Fau - Leunissen, K. M.; Leunissen Km Fau - Kitslaar, P. J.; Kitslaar, P. J., Early experience with stretch polytetrafluoroethylene grafts for haemodialysis access surgery: results of a prospective randomised study. (1078-5884 (Print)).
14. Tan, T. L. X.; May, K. K.; Robless, P. A.; Ho, P., Outcomes of Endovascular Intervention for Salvage of Failing Hemodialysis Access. *Annals of Vascular Diseases* **2011,** *4* (2), 87-92.
15. Nottelet, B.; Pektok, E.; Mandracchia, D.; Tille, J.-C.; Walpoth, B.; Gurny, R.; Moller, M., Factorial design optimization and in vivo feasibility of poly(e-caprolactone)-micro- and nanofiber-based small diameter vascular grafts. *Journal of Biomedical Materials Research Part A* **2008,** *89*, 865-75.
16. Pektok, E.; Nottelet, B.; Tille, J.-C.; Gurny, R.; Kalangos, A.; Moeller, M.; Walpoth, B. H., Degradation and healing characteristics of small-diameter poly(e-caprolactone) vascular grafts in the rat systemic arterial circulation. *Vascular Medicine* **2008,** *118*, 2563-70.
17. Jing, X.; Mi, H.-Y.; Salick, M. R.; Cordie, T. M.; Peng, X.-F.; Turng, L.-S., Electrospinning thermoplastic polyurethane/graphene oxide scaffolds for small diameter vascular graft applications. *Materials Science and Engineering: C* **2015,** *49*, 40-50.
18. Wang, H.; Feng, Y.; Fang, Z.; Yuan, W.; Khan, M., Co-electrospun blends of PU and PEG as potential biocompatible scaffolds for small-diameter vascular tissue engineering. *Materials Science and Engineering: C* **2012,** *32* (8), 2306-2315.

19. Doi, K.; Matsuda, T., Significance of porosity and compliance of microporous, polyurethane-based microarterial vessel on neoarterial wall regeneration. *Journal of Biomedical Materials Research* **1997,** *37*, 573-84.
20. Chaouat, M.; Le Visage, C.; Baille, W. E.; Escoubet, B.; Chaubet, F.; Mateescu, M. A.; Letourneur, D., A Novel Cross-linked Poly(vinyl alcohol) (PVA) for Vascular Grafts. *Advanced Functional Materials* **2008,** *18* (19), 2855-2861.
21. Cutiongco, M. F. A.; Anderson, D. E. J.; Hinds, M. T.; Yim, E. K. F., In vitro and ex vivo hemocompatibility of off-the-shelf modified poly(vinyl alcohol) vascular grafts. *Acta Biomater* **2015,** *25*, 97-108.
22. Cutiongco, M. F.; Kukumberg, M.; Peneyra, J. L.; Yeo, M. S.; Yao, J. Y.; Rufaihah, A. J.; Le Visage, C.; Ho, J. P.; Yim, E. K., Submillimeter Diameter Poly(Vinyl Alcohol) Vascular Graft Patency in Rabbit Model. *Frontiers in bioengineering and biotechnology* **2016,** *4*, 44.
23. Cutiongco, M. F.; Goh, S. H.; Aid-Launais, R.; Le Visage, C.; Low, H. Y.; Yim, E. K., Planar and tubular patterning of micro and nano-topographies on poly(vinyl alcohol) hydrogel for improved endothelial cell responses. *Biomaterials* **2016,** *84*, 184-95.
24. Nakazawa, Y.; Sato, M.; Takahashi, R.; Aytemiz, D.; Takabayashi, C.; Tamura, T.; Enomoto, S.; Sata, M.; Asakura, T., Development of small-diameter vascular grafts based on silk fibroin fibers from Bombyx mori for vascular regeneration. *Journal of Biomaterials Science* **2011,** *22*, 195-206.
25. Sato, M.; Nakazawa, Y.; Takahashi, R.; Tanaka, K.; Sata, M.; Aytemiz, D.; Asakura, T., Small-diameter vascular grafts of Bombyx mori silk fibroin prepared by a combination of electrospinning and sponge coating. *Materials Letters* **2010,** *64*, 1786-8.
26. Fukayama, T.; Takagi, K.; Tanaka, R.; Hatakeyama, Y.; Aytemiz, D.; Suzuki, Y.; Asakura, T., Biological reaction to small-diameter vascular grafts made of silk fibroin implanted in the abdominal aortae of rats. *Annals of Vascular Surgery* **2015,** *29*, 341-52.
27. Enomoto, S.; Sumi, M.; Kajimoto, K.; Nakazawa, Y.; Takahashi, R.; Takabayashi, C.; Asakura, T.; Sata, M., Long-term patency of small-diameter vascular graft made from fibroin, a silk-based biodegradable material. *Journal of Vascular Surgery* **2010,** *51*, 155-64.
28. Ballarin, F. M.; Caracciolo, P. C.; Blotta, E.; Ballarin, V. L.; Abraham, G. A., Optimization of poly(L-lactic acid)/segmented polyurethane electrospinning process for the production of bilayered small-diameter nanofibrous tubular structures. *Materials Science and Engineering C* **2014,** *42*, 489-99.
29. Sankaran, K. K.; Vasanthan, K. S.; Krishnan, U. M.; Sethuraman, S., Development and evaluation of axially aligned nanofibres for blood vessel tissue engineering. *Journal of Tissue Engineering and Regenerative Medicine* **2014,** *8*, 640-51.
30. Tara, S.; Kurobe, H.; Rocco, K. A.; Maxfield, M. W.; Best, C. A.; Yi, T.; Naito, Y.; Breuer, C. K.; Shinoka, T., Well-organized neointima of large-pore poly(L-lactic acid) vascular graft coated with poly(L-lactic-co-e-caprolactone) prevents calcific deposition compared to small-pore electrospun poly(L-lactic acid) graft in a mouse aortic implantation model. *Atherosclerosis* **2014,** *237*, 684-91.
31. Xie, Y.; Guan, Y.; Kim, S.-H.; King, M. W., The mechanical performance of weft-knitted/electrospun bilayer small diameter vascular prostheses. *Journal of the Mechanical Behavior of Biomedical Materials* **2016,** *61*, 410-8.
32. Montini-Ballarin, F.; Caracciolo, P. C.; Rivero, G.; Abraham, G. A., In vitro degradation of electrospun poly(L-lactic acid) segmented poly(ester urethane) blends. *Polymer Degradation and Stability* **2016,** *126*, 159-69.
33. Sankaran, K. K.; Krishnan, U. M.; Sethuraman, S., Axially aligned 3D nanofibrous grafts of PLA-PCL for small diameter cardiovascular applications. *Journal of Biomaterials Science, Polymer Edition* **2014,** *25* (16), 1791-1812.
34. Kirkwood, M. L.; Wang, G. J.; Jackson, B. M.; Golden, M. A.; Fairman, R. M.; Woo, E. Y., Lower limb revascularization for PAD using heparin-coated PTFE conduit. *Vascular and Endovascular Surgery* **2011,** *45* (4), 329-34.

35. Lin, P. H.; Bush, R. L.; Yao, Q.; Lumsden, A. B.; Chen, C., Evaluation of platelet deposition and neointimal hyperplasia of heparin-coated small-caliber ePTFE grafts in a canine femoral artery bypass model. *Journal of Surgical Research* **2004,** *118*, 45-52.
36. Zhu, A. P.; Ming, Z.; Jian, S., Blood compatibility of chitosan/heparin complex surface modified ePTFE vascular graft. *Applied Surface Science* **2005,** *241*, 485-92.
37. Thomas, A. C.; Campbell Gr Fau - Campbell, J. H.; Campbell, J. H., Advances in vascular tissue engineering. **2003,** (1054-8807 (Print)).
38. Nugent, M. J.; Higginbotham, C. L., Preparation of a novel freeze thawed poly(vinyl alcohol) composite hydrogel for drug delivery applications. *European journal of pharmaceutics and biopharmaceutics : official journal of Arbeitsgemeinschaft fur Pharmazeutische Verfahrenstechnik e.V* **2007,** *67* (2), 377-86.
39. Hassan, C. M.; Peppas, N. A., Structure and Morphology of Freeze/Thawed PVA Hydrogels. *Macromolecules* **2000,** *33* (7), 2472-2479.
40. Chu, K. C.; Rutt, B. K., Polyvinyl alcohol cryogel: an ideal phantom material for MR studies of arterial flow and elasticity. *Magnetic resonance in medicine* **1997,** *37* (2), 314-9.
41. Miranda, T. M. R.; Gonçalves, A. R.; Amorim, M. T. P., Ultraviolet-induced crosslinking of poly(vinyl alcohol) evaluated by principal component analysis of FTIR spectra. *Polymer International* **2001,** *50* (10), 1068-1072.
42. Figueiredo, K. C. S.; Alves, T. L. M.; Borges, C. P., Poly(vinyl alcohol) films crosslinked by glutaraldehyde under mild conditions. *Journal of Applied Polymer Science* **2009,** *111* (6), 3074-3080.
43. Guo, R.; Hu, C.; Li, B.; Jiang, Z., Pervaporation separation of ethylene glycol/water mixtures through surface crosslinked PVA membranes: Coupling effect and separation performance analysis. *Journal of Membrane Science* **2007,** *289* (1), 191-198.
44. Wan, W. K.; Campbell, G.; Zhang, Z. F.; Hui, A. J.; Boughner, D. R., Optimizing the tensile properties of polyvinyl alcohol hydrogel for the construction of a bioprosthetic heart valve stent. *Journal of biomedical materials research* **2002,** *63* (6), 854-61.
45. Fathi, E.; Nassiri, S. M.; Atyabi, N.; Ahmadi, S. H.; Imani, M.; Farahzadi, R.; Rabbani, S.; Akhlaghpour, S.; Sahebjam, M.; Taheri, M., Induction of angiogenesis via topical delivery of basic-fibroblast growth factor from polyvinyl alcohol-dextran blend hydrogel in an ovine model of acute myocardial infarction. *Journal of tissue engineering and regenerative medicine* **2013,** *7* (9), 697-707.
46. Kobayashi, M.; Chang, Y. S.; Oka, M., A two year in vivo study of polyvinyl alcohol-hydrogel (PVA-H) artificial meniscus. *Biomaterials* **2005,** *26* (16), 3243-8.
47. Yang, W.-H.; Smolen, V. F.; Peppas, N. A., Oxygen permeability coefficients of polymers for hard and soft contact lens applications. *Journal of Membrane Science* **1981,** *9* (1), 53-67.
48. Ding, J.; He, R.; Zhou, G.; Tang, C.; Yin, C., Multilayered mucoadhesive hydrogel films based on thiolated hyaluronic acid and polyvinylalcohol for insulin delivery. *Acta biomaterialia* **2012,** *8* (10), 3643-51.
49. Wan, W. B., A. Dawn; Yang, Lifang; Mak, Helium, Poly(vinyl alcohol) cryogels for biomedical applications. *Advances in Polymer Science* **2014,** *263*, 283-316.
50. Peijs, T.; van Vught, R. J. M.; Govaert, L. E., Mechanical properties of poly(vinyl alcohol) fibres and composites. *Composites* **1995,** *26* (2), 83-90.
51. Mantovani, D.; Castonguay, M.; Pageau, J. F.; Fiset, M.; Laroche, G., Ammonia RF-Plasma Treatment of Tubular ePTFE Vascular Prostheses. *Plasmas and Polymers* **1999,** *04* (2-3), 207-228.
52. Dai, Z.; Ronholm, J.; Tian, Y.; Sethi, B.; Cao, X., Sterilization techniques for biodegradable scaffolds in tissue engineering applications. *Journal of tissue engineering* **2016,** *7*, 2041731416648810.
53. Holy, C. E.; Cheng, C.; Davies, J. E.; Shoichet, M. S., Optimizing the sterilization of PLGA scaffolds for use in tissue engineering. *Biomaterials* **2001,** *22* (1), 25-31.
54. Bongrand, P., Specific and Nonspecific Interactions in Cell Biology. *Journal of Dispersion Science and Technology* **1998,** *19* (6-7), 963-978.
55. Pierres, A.; Benoliel, A.-M.; Bongrand, P., Studying receptor-mediated cell adhesion at the single molecule level. *Cell Adhesion and Communication* **1998,** *5* (5), 375-395.

56. Barczyk, M.; Carracedo, S.; Gullberg, D., Integrins. *Cell and Tissue Research* **2009,** *339* (1), 269.
57. Kanchanawong, P.; Shtengel, G.; Pasapera, A. M.; Ramko, E. B.; Davidson, M. W.; Hess, H. F.; Waterman, C. M., Nanoscale architecture of integrin-based cell adhesions. *Nature* **2010,** *468* (7323), 580-4.
58. Schultz, K.; Kyburz, K.; Anseth, K., Measuring dynamic cell-material interactions and remodeling during 3D human mesenchymal stem cell migration in hydrogels. *Proceedings of the National Academy of Sciences of the United States of America* **2015,** *112* (29), E3757.
59. Andalib, M. N.; Lee, J. S.; Ha, L.; Dzenis, Y.; Lim, J. Y., Focal adhesion kinase regulation in stem cell alignment and spreading on nanofibers. *Biochemical and Biophysical Research Communications* **2016,** *473* (4), 920-5.
60. Bennett, V., Cell differentiation. *Current Opinion in Cell Biology* **2008,** *20* (6), 607-8.
61. Tan, S. H.; Nguyen, N.-T.; Chua, Y. C.; Kang, T. G., Oxygen plasma treatment for reducing hydrophobicity of a sealed polydimethylsiloxane microchannel. *Biomicrofluidics* **2010,** *4* (032204), 1-8.
62. Ino, J. M.; Chevallier, P.; Letourneur, D.; Mantovani, D.; Le Visage, C., Plasma functionalization of poly(vinyl alcohol) hydrogel for cell adhesion enhancement. *Biomatter* **2013,** *3* (4).
63. Pavli, P.; Petrou, P. S.; Douvas, A. M.; Dimotikali, D.; Kakabakos, S. E.; Argitis, P., Protein-resistant cross-linked poly(vinyl alcohol) micropatterns via photolithography using removable polyoxometalate photocatalyst. *ACS applied materials & interfaces* **2014,** *6* (20), 17463-73.
64. Pourciel, M. L.; Launay, J.; Sant, W.; Conédéra, V.; Martinez, A.; Temple-Boyer, P., Development of photo-polymerisable polyvinyl alcohol for biotechnological applications. *Sensors and Actuators B: Chemical* **2003,** *94* (3), 330-336.
65. Anderson, D. E.; Glynn, J. J.; Song, H. K.; Hinds, M. T., Engineering an endothelialized vascular graft: a rational approach to study design in a non-human primate model. *PloS one* **2014,** *9* (12), e115163.
66. Cutiongco, M. F. A.; Chua, B. M. X.; Neo, D. J. H.; Rizwan, M.; Yim, E. K. F., Functional differences between healthy and diabetic endothelial cells on topographical cues. (1878-5905 (Electronic)).
67. Calderwood, D. A.; Shattil, S. J.; Ginsberg, M. H., Integrins and Actin Filaments: Reciprocal Regulation of Cell Adhesion and Signaling. *Journal of Biological Chemistry* **2000,** *275* (30), 22607-22610.
68. Granger, D. S., E, Leukocyte-Endothelial Cell Adhesion. In *Inflammation and the Microcirculation*, Morgan & Claypool Life Sciences: San Rafael (CA), 2010.
69. Yoganarasimha, S.; Trahan, W. R.; Best, A. M.; Bowlin, G. L.; Kitten, T. O.; Moon, P. C.; Madurantakam, P. A., Peracetic acid: a practical agent for sterilizing heat-labile polymeric tissue-engineering scaffolds. *Tissue engineering. Part C, Methods* **2014,** *20* (9), 714-23.
70. Valente, T. A.; Silva, D. M.; Gomes, P. S.; Fernandes, M. H.; Santos, J. D.; Sencadas, V., Effect of Sterilization Methods on Electrospun Poly(lactic acid) (PLA) Fiber Alignment for Biomedical Applications. *ACS applied materials & interfaces* **2016,** *8* (5), 3241-9.
71. Gogolewski, S.; Mainil-Varlet, P., Effect of thermal treatment on sterility, molecular and mechanical properties of various polylactides. 2. Poly(L/D-lactide) and poly(L/DL-lactide). *Biomaterials* **1997,** *18* (3), 251-5.
72. Volland, C.; Wolff, M.; Kissel, T., The influence of terminal gamma-sterilization on captopril containing poly(d,l-lactide-co-glycolide) microspheres. *Journal of Controlled Release* **1994,** *31* (3), 293-305.
73. Zislis, T.; Mark, D. E.; Cerbas, E. L.; Hollinger, J. O., Scanning electron microscopic study of cell attachment to biodegradable polymer implants. *The Journal of oral implantology* **1989,** *15* (3), 160-7.
74. Cox, M. M.; Battista, J. R., Deinococcus radiodurans - the consummate survivor. *Nature reviews. Microbiology* **2005,** *3* (11), 882-92.
75. Lambert, P. A., Radiation Sterilization. In *Russell, Hugo & Ayliffe's*, Wiley-Blackwell: 2013; pp 294-305.
76. Gilding, D. K.; Reed, A. M., Biodegradable polymers for use in surgery—polyglycolic/poly(actic acid) homo- and copolymers: 1. *Polymer* **1979,** *20* (12), 1459-1464.

77. Clough, R. L., High-energy radiation and polymers: A review of commercial processes and emerging applications. *Nuclear Instruments and Methods in Physics Research Section B: Beam Interactions with Materials and Atoms* **2001,** *185* (1), 8-33.
78. Brennen Md Fau - O'Brien, B. M.; O'Brien, B. M., Patency rates in end to side anastomoses in the rabbit. (0007-1226 (Print)).
79. Li, R.; Lan, B.; Zhu, T.; Yang, Y.; Wang, M.; Ma, C.; Chen, S., Establishment of an Animal Model of Vascular Restenosis with Bilateral Carotid Artery Grafting. *Medical Science Monitor : International Medical Journal of Experimental and Clinical Research* **2014,** *20*, 2846-2854.
80. Jackson, Z. S.; Ishibashi H Fau - Gotlieb, A. I.; Gotlieb Ai Fau - Langille, B. L.; Langille, B. L., Effects of anastomotic angle on vascular tissue responses at end-to-side arterial grafts. (0741-5214 (Print)).
81. Assmann, A.; Akhyari P Fau - Delfs, C.; Delfs C Fau - Flogel, U.; Flogel U Fau - Jacoby, C.; Jacoby C Fau - Kamiya, H.; Kamiya H Fau - Lichtenberg, A.; Lichtenberg, A., Development of a growing rat model for the in vivo assessment of engineered aortic conduits. (1095-8673 (Electronic)).
82. Tiwari, A.; Cheng, K. S.; Salacinski, H.; Hamilton, G.; Seifalian, A. M., Improving the patency of vascular bypass grafts: The role of suture materials and surgical techniques on reducing anastomotic compliance mismatch. *European Journal of Vascular and Endovascular Surgery* **2003,** *25* (4), 287-295.
83. Byrom, M. J.; Bannon, P. G.; White, G. H.; Ng, M. K., Animal models for the assessment of novel vascular conduits. *J Vasc Surg* **2010,** *52* (1), 176-95.
84. Tomiyama, Y.; Yoshinaga, K.; Fujii, S.; Ochi, N.; Inoue, M.; Nishida, M.; Aziki, K.; Horie, T.; Katoh, C.; Tamaki, N., Accurate quantitative measurements of brachial artery cross-sectional vascular area and vascular volume elastic modulus using automated oscillometric measurements: comparison with brachial artery ultrasound. *Hypertension research : official journal of the Japanese Society of Hypertension* **2015,** *38* (7), 478-84.
85. Matsumoto, T. O., Eijiro; Shirono, Takahiro; Sho, Eiketsu; Masuda, Hirotake; Sato, Masaaki, Flow-induced changes in dimensions and mechanical properties of rabbit common carotid arteries. *JSME International Journal* **2005,** *48* (4), 477-483.
86. Salzer, D. A.; Medeiros, P. J.; Craen, R.; Shoemaker, J. K., Neurogenic-nitric oxide interactions affecting brachial artery mechanics in humans: roles of vessel distensibility vs. diameter. *American Journal of Physiology - Regulatory, Integrative and Comparative Physiology* **2008,** *295* (4), R1181-R1187.
87. Wang, P.; Shu, Z.; He, L.; Wang, Y.; Cui, X.; Yu, J.; Lu, J.; Gao, D., *The Viability, Structure, and Mechanical Properties of Cryopreserved Rabbit Carotid Artery*. 2005; Vol. 3, p 85-95.
88. Bank, A. J.; Kaiser, D. R.; Rajala, S.; Cheng, A., In vivo human brachial artery elastic mechanics: effects of smooth muscle relaxation. *Circulation* **1999,** *100* (1), 41-7.
89. Green, S. I.; Schajer, G. S.; Parker, D. R.; Post, A. J.; Hsiang, Y. N., In vivo measurement of arterial pre-tension. *Medical & biological engineering & computing* **1995,** *33* (6), 826-9.
90. Fung, Y. C.; Fronek, K.; Patitucci, P., Pseudoelasticity of arteries and the choice of its mathematical expression. *The American journal of physiology* **1979,** *237* (5), H620-31.